The climate of the Mediterranean region in future climate projections

Serge Planton, Piero Lionello, Vincenzo Artale, Rolland Aznar, Adriana Carrillo, Jeanne Colin, Letizia Congedi, Clotilde Dubois, Alberto Elizalde, Silvio Gualdi, Elke Hertig, Jucundus Jacobeit, Gabriel Jordà, Laurent Li, Annarita Mariotti, Claudio Piani, Paolo Ruti, Emilia Sanchez-Gomez, Gianmaria Sannino, Florence Sevault, Samuel Somot, Michael Tsimplis

Angaben zur Veröffentlichung / Publication details:

Planton, Serge, Piero Lionello, Vincenzo Artale, Rolland Aznar, Adriana Carrillo, Jeanne Colin, Letizia Congedi, et al. 2012. "The climate of the Mediterranean region in future climate projections." In *The Climate of the Mediterranean Region: From the past to the future*, edited by Piero Lionello, 449–502. Amsterdam: Elsevier. https://doi.org/10.1016/b978-0-12-416042-2.00008-2.

8 The Climate of the Mediterranean Region in Future Climate Projections

Serge Planton[a], Piero Lionello[b], Vincenzo Artale[c], Rolland Aznar[d], Adriana Carrillo[c], Jeanne Colin[a], Letizia Congedi[b], Clotilde Dubois[a], Alberto Elizalde[e], Silvio Gualdi[f], Elke Hertig[g], Jucundus Jacobeit[g], Gabriel Jordà[h], Laurent Li[i], Annarita Mariotti[c], Claudio Piani[j], Paolo Ruti[c], Emilia Sanchez-Gomez[k], Gianmaria Sannino[c], Florence Sevault[a], Samuel Somot[a], Michael Tsimplis[l]

[a]Centre National de Recherches Météorologiques—Groupe d'études de l'Atmosphère Météorologique, Météo-France, Toulouse, France, [b]Department of Material Science, University of Salento, Salento, Italy, [c]ENEA, Rome, Italy, [d]Área de Medio Físico, Dirección de Relaciones Institucionales e Innovación, Tecnológica, Puertos del Estado, Madrid, Spain, [e]Max Planck Institute for Meteorology, Hamburg, Germany, [f]Instituto Nazionale di Geofisica e Vulcanologia, Bologna, Italy, [g]Institute of Geography, University of Augsburg, Augsburg, Germany, [h]Institut Mediterrani d'Estudis Avançats, Esporles, Spain, [i]Laboratoire de Météorologie Dynamique, Institut Pierre Simon Laplace, Paris, France, [j]International Centre for Theoretical Physics, Trieste, Italy, [k]Centre Européen de Recherche et de Formation Avancée en Calcul Scientifique, Toulouse, France, [l]Ocean Observing and Climate, National Oceanography Centre, Southampton, UK

8.1 Introduction

Future climate change over the Mediterranean is investigated by means of climate model simulations covering the twenty-first century. These simulations follow different emission scenarios of gases that are linked to human activities and are known to have an impact on climate through the greenhouse radiative effect (CO_2, CH_4, N_2O, and other trace gases). In addition, the scenarios take into account the emission of aerosols (airborne solid or liquid particles) that influence the climate through reflection and absorption of solar radiation and by changing cloud radiative properties.

The Climate of the Mediterranean Region. DOI: 10.1016/B978-0-12-416042-2.00008-2

The emission scenarios are those prescribed by the Intergovernmental Panel on Climate Change (IPCC) Working group III (WGIII), which is in charge of the assessment of options for mitigating climate change (IPCC SRES, 2000). Emission scenarios are images of possible future developments, but they are not predictions, since they are based on many aspects of social systems that are unpredictable at a multidecadal timescale (e.g., population growth, socioeconomic development, and technological progress). Starting from an ensemble of 40 emission scenarios developed by six modeling groups, the WGIII proposed four scenario families referred to as SRES A1, A2, B1, and B2, the first being itself divided into subgroups A1FI, A1T, and A1B according to their technological emphasis. A short description of the SRES emission scenarios is given in the "Summary for Policymakers" of the IPCC WG1 Fourth Assessment Report (IPCC-AR4) (IPCC, 2007). Approximate CO_2 equivalent concentrations corresponding to the computed radiative forcing due to anthropogenic greenhouse gases in 2100 for the SRES B1, B2, A1B, and A2 scenarios referred in this chapter are about 600, 800, 850, and 1250 ppm, respectively.

The climate-change simulations are first performed with general circulation models (GCMs), coupling the atmosphere, land areas, and the ocean at the global scale (also designated as AOGCMs). These models may include other components of the climate system (e.g., sea-ice and continental hydrology) and some biogeochemical processes (e.g., stratospheric ozone and carbon cycle). Starting from initial conditions for the atmosphere and the ocean that are representative of the present climate, each model is integrated to calculate climate evolution until the end of twenty-first century. In each simulation, concentrations of greenhouse gases and aerosol load are prescribed in agreement with a particular SRES emission scenario for the future. At the international level, the Working Group on Coupled Modelling from the World Climate Research Program, coordinates the Coupled Models Intercomparison Project (CMIP), which gives a common framework for the climate-change simulations performed by different climate research groups. The third phase of CMIP (CMIP3) involved 16 groups in 11 countries with 23 global AOGCMs and served as a basis of AR4. Some results from this ensemble of simulations concerning the Mediterranean area are reported in this chapter.

For the analysis of regional climate change, the AOGCM simulations may be downscaled dynamically by means of limited area regional climate models (RCMs) and varying resolution atmospheric general circulation models (AGCMs) or statistically using appropriate techniques. Over the Mediterranean domain, RCMs may be only atmospheric models (ARCMs) or atmospheric models coupled with a high-resolution Mediterranean Sea model (AORCMs). Several European projects have produced coordinated ensembles of simulations with several RCMs. Within the context of the PRUDENCE project (Christensen and Christensen, 2007), 4 high-resolution atmosphere-only GCMs and 10 RCMs were used in different combinations and two different SRES scenarios (A2 and B2) but downscaled climate-change simulations from only three different AOGCMs. As part of the ENSEMBLES project (Goodess et al., 2009), the combination of different models was much wider, since it included 8 AOGCMs and 16 RCMs. At the end of the CIRCE project (2007–2011), a new ensemble of several AORCMs will become available. Some results obtained

from these ensembles of simulations are detailed in this chapter. Different statistical techniques have also been applied to downscale AORCMs projections over the Mediterranean area. One of the most recent applications is that of Hertig and Jacobeit (2008) using a multiple-regression analysis and a canonical-correlation analysis (CCA). Further details of some results from this study are given below.

In addition, we also consider a few scenario simulations aimed at analyzing the impact of climate change on the Mediterranean Sea itself, using a high-resolution model of the sea constrained with the outputs of some high-resolution atmosphere-only climate-change scenarios. We will report some results from one of these simulations performed recently.

8.2 Investigating Methods

There are three main ways to develop methods that are used for climate-change assessment at the regional scale. The first concerns the resolution of the RCMs and the varying resolution of AGCMs. It was commonly ~50km over the Mediterranean area at the beginning of the 2000s (see PRUDENCE project, Christensen and Christensen, 2007), but now reach resolutions of ~20km over the whole domain (see ENSEMBLES and Climate Change and Impact Research: the Mediterranean Environment [CIRCE] projects) or even ~10km over some specific part of the region. The second way is the improvement of RCMs and downscaling techniques. One domain of development of RCMs concerns the coupling of different components of the climate system at the regional scale. The first step was the coupling of a Mediterranean Sea model with an RCM (see CIRCE project), with optionally coupling to include a river-routing component. The third method of development is the construction of multimodel ensembles of simulations within the context of scientific projects aiming at a better characterization of the uncertainties of the projections. The PRUDENCE, ENSEMBLES, and CIRCE projects are examples of such constructions, with an increasing number of GCMs and RCMs within the two first and an investigation of coupled atmosphere–Mediterranean Sea high-resolution models for the third one. In this section, we present some results on the impact of model resolution and of high-resolution coupling on the simulated climate change. The application of ensembles of simulations for the evaluation of the uncertainties of the projections over the Mediterranean region will be presented in Section 8.5.

8.2.1 Impact of Resolution

Some results on the impact of RCM resolution have been reported by Gao et al. (2006) by the application of the RegCM model at two different horizontal resolutions (50 and 20km) for present climate conditions (1961–1990) and for a 30-year period at the end of this century (2071–2100) under the SRES A2 scenario. They show the impact of resolution on the structure of the mean precipitation change signal that presents fine-scale structures linked to the topography more pronounced during the cold season. For instance, in winter, the increase of southwesterly winds over the Alps induces an increase in precipitation south of the Alps and no change in the

north. The same kind of topographical influence is also reported for maximum dry-spell length and maximum 5-day precipitation.

Apart from these small-scale changes in the fine structure of the precipitation field, the results of the CMIP3 (GCMs) and PRUDENCE and ENSEMBLES projects (RCMs), summarized in the IPCC-AR4, show that qualitatively in most cases the impact of the model resolution does not dramatically change the climate-change impact over the Mediterranean area. Large-scale spatial pattern and seasonal changes are mostly in agreement between GCMs and RCMs over the Mediterranean area for wind, temperature, and precipitation variables. Sanchez-Gomez et al. (2009) compared the CMIP3 GCMs and the ENSEMBLES RCMs regarding the Mediterranean Sea water-budget evolution under the SRES A1B scenario. The results obtained are generally similar for most of the water-budget terms, except for the river-discharge response that seems to be unrealistic in GCMs. Despite these differences found in the river-discharge terms, they concluded that the total freshwater deficit for the period 2070–2099 related to 1950–1999 presents a mean increase of +40% for both RCMs and GCMs (see also section 8.4.2).

Elguindi et al. (2010) also tackled the issue of the impact of the horizontal resolution but using a completely different method. They used the same global AGCM ARPEGE-Climat, but with different spatial resolutions and keeping the rest of the model setup unchanged (e.g., the physical parameterizations are unchanged). They explored three resolutions: TL63 (1.9 × 1.9°), TL159 (1.125 × 1.125°), and TL359 (0.5 × 0.5°) for time slices in the present (1979–2002) and future (2046–2070, A2) climates. Their work is really a unique opportunity to isolate and study the effects of resolution on simulating the Mediterranean climate and its response to climate change. In addition, the low-resolution (LowRes) model corresponds to the former CNRM-CM model used for CMIP3, the medium-resolution (MedRes) model to the ERA40 reanalysis resolution, and the high-resolution (HighRes) model to the state-of-art RCMs used for the forthcoming CORDEX (COordinated Regional climate Downscaling EXperiment) simulation exercise. They mainly looked at the near-surface temperature, the precipitation, and the Mediterranean Sea water-budget components. For the present climate, the model performance improves significantly with increased resolution, especially in regions with mountainous terrain for precipitation and for the river discharge. But only the HighRes is able to simulate a Mediterranean Sea water budget in agreement with the observations; the two other models show significant underestimation. However, the impact of the resolution on the 2 m temperature bias is weak. Concerning the response to climate change, the change in resolution does not qualitatively alter the impact of climate change on the climate variables. It is worth noting that for temperature, the LowRes model shows the most extreme response for the future climate. Changes in precipitation over land do not show a clear signal of the impact of the resolution. However, the resolution does show an impact on the net evaporation changes over the sea (evaporation–precipitation (E − P)), for which an increased resolution leads to an enhanced increased net evaporation in future climate, from +15% in LowRes to +22% in HighRes. In addition, as in Sanchez-Gomez et al. (2009), the resolution also shows an impact on the Mediterranean river discharge, for which the decrease is stronger

when the resolution is lower, going from −11% in HighRes to −28% in LowRes. If we add the contribution of the Black Sea freshwater input to the Mediterranean rivers, the HighRes shows a 15% decrease in total freshwater input, whereas LowRes shows a 37% decrease enhancing the model spread. The MedRes results are between those of the two other models. The effect of the resolution on the evaporation (the higher the resolution, the stronger the change in evaporation) compensates for the effect on the river discharge (the higher the resolution, the weaker the decrease in river discharge), and the overall Mediterranean Sea water budget does not show a clear signal of the resolution (about −40% in both LowRes and HighRes).

8.2.2 Impact of Regional Coupling

After some preliminary investigations—in which a coupled atmosphere–ocean-wave model was implemented in the Mediterranean Sea and demonstrated the sensitivity of the short-scale evolution of the system to the coupling mechanisms (Lionello et al., 2003a) and the consequent improvement of the SST annual cycle, in 2005—a first high-resolution and fully interactive atmosphere–ocean RCM dedicated to the study of the Mediterranean climate and sea variability was set up (Somot, 2005). This model, already mentioned in the first Mediterranean Climate Variability and Predictability (MedCLIVAR) book (Li et al., 2006), was published following the study of a SRES A2 scenario performed with this new numerical tool (Somot et al., 2008). In this study, the authors evaluate the impact of the regional air–sea coupling comparing the AORCM simulation with a twin ARCM simulation.

Note that in this AORCM, the regional atmosphere is coupled to a complex land-surface scheme ISBA, but the river discharge produced by this surface scheme is not coupled to the regional ocean. It is an atmosphere–land–ocean regional coupled climate model but without the land-to-ocean coupling. The external forcings of such a model are, consequently, the sea-surface temperature (SST) outside the Mediterranean area, the temperature–salinity (T–S) characteristics of the near-Atlantic Ocean, and the river discharge that comes from a previously run uncoupled regional atmosphere model.

From a first analysis, we observe that the climate-change. However, the AORCM significantly amplifies the climate-change signal over large parts of Europe at the end of the twenty-first century (2070–2099 versus 1961–1990); the warming is higher in all seasons and in many areas of Europe (up to 25% of the signal), winters are wetter over northern Europe, and the summers are drier over southern and eastern Europe (up to 50% of the signal). These differences are highly significant, and the authors concluded that the choice between coupled and noncoupled regional models could be an additional source of uncertainty when evaluating the climate-change response over Europe. Among other factors, the response of the Mediterranean SST to climate change, better simulated by the high-resolution Mediterranean Sea model of the AORCM, seems to be the predominant factor responsible for the described differences. The pioneer work with a high-resolution coupled AORCM for the Mediterranean area opened the way for the European CIRCE project, which includes six different AORCMs dedicated to the study of the Mediterranean climate change.

8.3 Projections of Future Climate

8.3.1 Mean Climate

Giorgi and Lionello (2008) made a review of climate-change projections over the Mediterranean region based on a large ensemble of 17 global climate-change simulations extracted from the MGME (Multi Global Model Ensemble) stored at the Program for Climate Model Diagnosis and Intercomparison (PCMDI; http://www-pcmdi.llnl.gov), an ensemble of simulations analyzed in the AR4. A robust and large warming is projected, with a maximum in the summer season. Figure I.20 (top) shows the ensemble temperature increase of the 2071–2100 period with respect to the 1961–2100 period for the A1B scenario. In summer (JJA), values reach 3–4°C over the sea, grow further to 4–5°C in inland areas, and have maxima higher than 5°C in the Sahara and Middle East. Also, other seasons present substantial temperature increases—2–3°C in winter and spring, and 3–4°C in autumn. With respect to A1B, changes would be about half a degree higher for the A2 scenario and 1 degree lower for the B1 scenario. Climate change would affect land areas more than the sea, with differences between the Mediterranean Sea and the surrounding lands between 0.4°C and 0.6°C, reaching 0.9°C in summer. Figure I.20 (bottom) shows the ensemble change of precipitation for the same periods and scenario as for temperature. The reduction in precipitation is smallest in winter, where it varies from no change in the northern Mediterranean to a 40% reduction in the south. In spring and fall, the reductions of precipitation vary between 10% and 40%. The average value of the large summer reduction is in the range 25–30%, but some areas in the northeast and the south show a decrease that is larger than 50%. For most model simulations, the mean annual precipitation decrease, when averaged over the whole basin, is larger over sea than over land, except in winter. As for temperature, precipitation changes for the B1 (A2) scenario are smaller (larger) than for the A1B scenario. When averaged over the whole Mediterranean region in the A2 scenario, precipitation reductions reach 20–30% during the intermediate seasons and up to 30–40% in summer. Both signals in precipitation and temperature are projected to become progressively more severe during the twenty-first century.

Beside changes of mean values, climate projections also include important changes of variability. Both temperature and precipitation distributions present simultaneously a considerable shift and deformation, becoming broader in future climate scenarios. Increased interannual variability, especially in summer, along with the mean warming, would lead to a greater occurrence of extremely high temperature events. Similarly, for precipitation, the decrease of mean precipitation and the increased frequency of large negative anomalies would increase the intensity and frequency of droughts (Giorgi and Coppola, 2009).

A substantial consensus exists among climate simulations carried out with both RCMs and GCMs, as well as between the more recent analysis and previous generations of model projections (see Christensen and Christensen (2007) and Giorgi and Coppola (2009) for PRUDENCE RCM simulations). Here, we present new results obtained with an ensemble of RCM simulations performed in the context

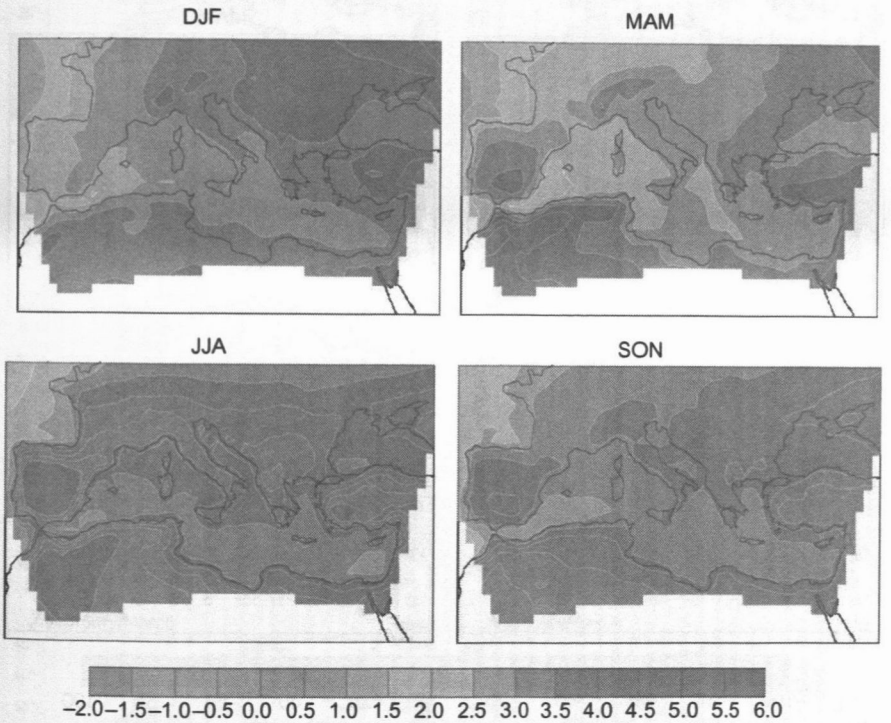

Figure 8.1 Seasonal (DJF, MAM, JJA, SON) map of temperature climate change (K) as resulting from an ensemble of RCMs. The maps show the differences between the 2071–2100 period of the A1B scenario and the reference period 1961–1990.

of the ENSEMBLES project (Figures 8.1 and 8.2). For this study, an ensemble has been selected with simulation domains covering the whole Mediterranean basin. The ensemble consists of six members: RACMO, RCA, REMO, RegCM driven by the ECHAM-r3 global model, CLM, and HadRM3 driven by HadCM3. In order to balance the effect of the two GCMs, a double weight has been give to the RCMs driven by HadCM3. For precipitation, Figure 8.2 shows differences expressed as a percentage of the mean value of the reference period.

In agreement with the above-mentioned studies and with the results reported in Section 8.2.1, there are broad similarities between temperature and precipitation changes simulated by GCMs (Figure I.20) and by the ENSEMBLES RCMs (Figures 8.1 and 8.2). Over land, the warming for RCMs is roughly within the range of 2.5–3.5°C in winter and 4–5°C in summer. Over the sea, the warming is roughly within the range of 2–3.5°C with a lower seasonal dependence. Precipitation changes simulated by RCMs also generally agree with those simulated by GCMs, with a substantial future drying in all seasons and areas of the Mediterranean region, except in winter in the northern part. The actual meaning of a further summer reduction when precipitation is very low (if not absent) should probably not be emphasized.

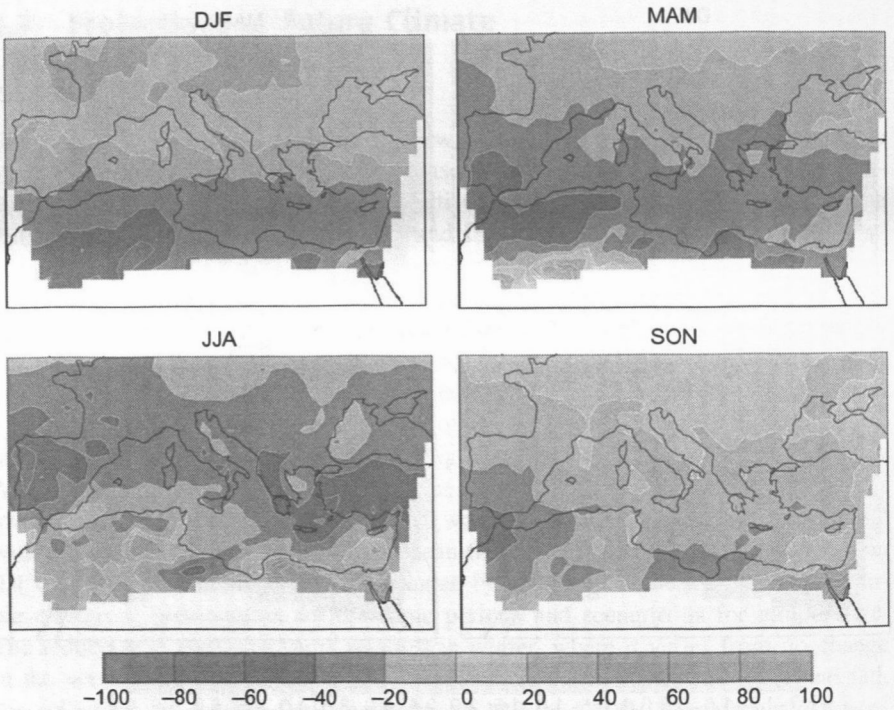

Figure 8.2 Same as Figure 8.1, except that it shows climate change for the precipitation signal (percent of the value in the reference period).

The main conclusion from this comparison RCM with GCM is that warming and drying of the Mediterranean region at the end of the twenty-first century is very likely, but actual values and their detailed spatial distribution remain uncertain, as they depend on the modeling tools (see Section 8.2).

A statistical downscaling approach has been applied to investigate climate change over the Mediterranean domain (Hertig and Jacobeit, 2008). Figure 8.3 shows its results for Mediterranean precipitation changes in the period 2071–2100 in relation to the period 1990–2019 for the main rainy season from October to May. They are derived from statistical downscaling models (based on CCA techniques) linking highly resolved gridded data of Mediterranean precipitation to large-scale atmospheric predictors (1000 and 500 hPa geopotential height fields as well as 1000 hPa specific humidity).

For the SRES B2 scenario, the assessments indicate a shortening of the wet season and at the same time an increase in rainfall amount during high winter for the western and northern Mediterranean regions. Thus, for these regions, precipitation decreases dominate in autumn and spring. In contrast, the eastern and southern parts of the Mediterranean area reveal mainly negative precipitation changes throughout the period from October to May. In this context, circulation dynamics point to

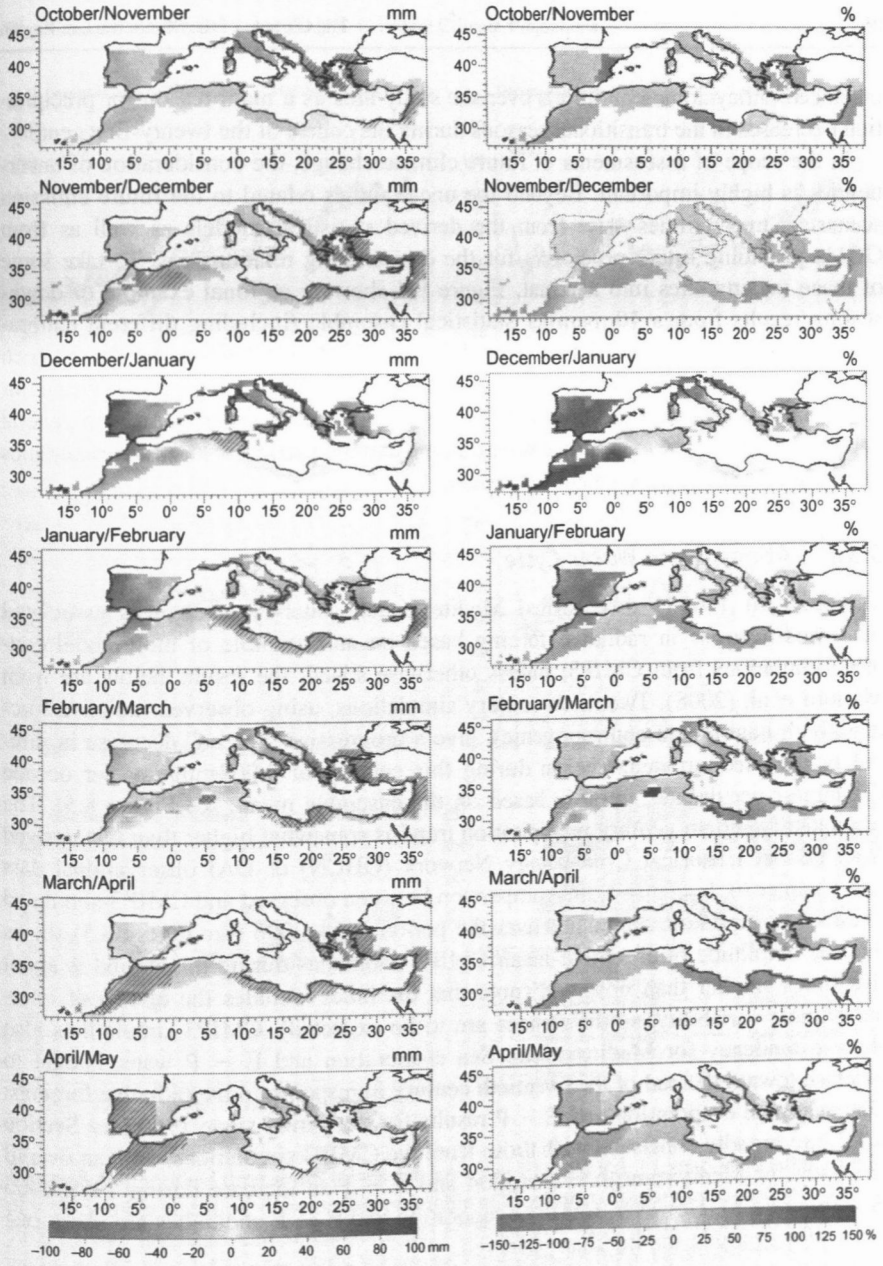

Figure 8.3 Changes of Mediterranean precipitation according to the statistical downscaling assessments using ECHAM4/OPYC3 predictors (1000 and 500 hPa geopotential heights, 1000 hPa specific humidity) under SRES B2 scenario assumptions—differences of the mean 2-month precipitation between the periods 2071–2100 and 1990–2019 in millimeters (left) and percentages in relation to the mean of the earlier period (right). The statistical downscaling technique used was CCA. Transverse hatching: signal:noise ratio >1 (confidence level, 68.3%); cross hatching: signal:noise ratio >1.96 (confidence level, 95%).
Source: Adapted from Hertig and Jacobeit (2008).

enhanced anticyclonic conditions over the study area as a main reason for precipitation decreases in the transitional seasons during the course of the twenty-first century.

In the scope of assessments of future climate change, the consideration of uncertainties is highly important. Beyond the uncertainties related to the future emission scenarios, uncertainties arise from the derived statistical models as well as from GCMs providing future predictors for the downscaling relationships. To take some of these uncertainties into account, Figure 8.4 shows a regional example of downscaling results from a 10-member statistical ensemble (including different calibration and verification periods) for five different GCM simulations. As can be seen in Figure 8.4, all the different assessments include a long-term positive trend for high-winter precipitation in this case. While this long-term progression is in general agreement, short- and medium-term variations and the particular trend characteristics may differ from one assessment to another.

8.3.2 Atmospheric Water Cycle

Mariotti et al. (2008) also studied Mediterranean water-cycle changes associated with modifications in radiative forcing based on an ensemble of multimodel coupled simulations from CMIP3; unless otherwise stated, the results below are from Mariotti et al. (2008). Twentieth-century simulations, using observed radiative forcings (both natural and anthropogenic), give a progressive "forced" decrease in rainfall in the Mediterranean region during this century of 0.007 mm/day per decade (2.5 mm/yr per decade; trend is based on the ensemble mean; see Figure 8.5). The simulated twentieth-century precipitation trend is somewhat higher than that derived from Global Historical Climatology Network (GHCN) or DAI observational data (see Chapter 6). In contrast, the comparison between observed and CMIP3-simulated "forced" precipitation anomalies over the period 1958–2006 (see Figure 8.5) shows that the amplitude of ensemble-mean CMIP3 anomalies during this period is about five times smaller than observed (note that the latter includes the effects of internal climate variability, so differences are to be expected). CMIP3 simulations also show a tendency for Mediterranean Sea evaporation and E − P water budget to increase toward the end of the twentieth century in response to the radiative forcings. Observational evaporation and E − P results for the period since 1960 (see Section 6.4.2) are broadly consistent with those from the CMIP3 simulations, with an overall tendency for Mediterranean evaporation and E − P to increase during 1958–2006 (see Figure 8.5). However, CMIP3 evaporation and E − P anomalies are about one order of magnitude smaller than observed.

Based on an ensemble of CMIP3 twenty-first-century SRES A1B emission scenario simulations, Mariotti et al. (2008) showed that the above-mentioned simulated twentieth-century precipitation decrease would be followed by a rapid drying from 2020 onward (precipitation decrease is 0.02 mm/day per decade or 7.2 mm/yr per decade). This amounts to roughly 15% less precipitation in 2070–2099 as compared with 1950–2000, and an 8% decrease already by 2020–2049 as the "forced" response to increased greenhouse gases (these results are in the ballpark of those from other studies, such as Giorgi and Lionello, 2008 and IPCC, 2007).

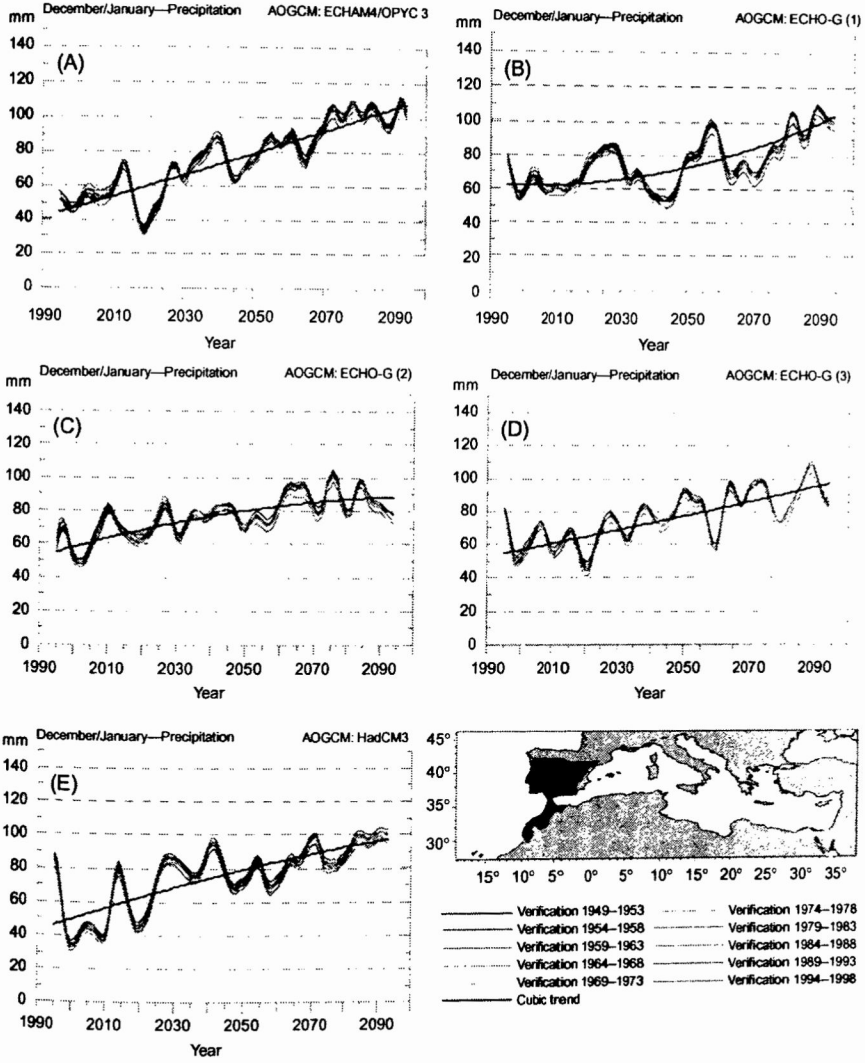

Figure 8.4 Smoothed time series (Gaussian low-pass filter period, 11 years) and cubic trends of a 10-member statistical downscaling ensemble of December–January precipitation 1990–2100 for five different GCM simulations: (A) ECHAM4/OPYC3; (B–D) ECHO-G ensemble members; (E) HadCM3 under SRES B2 scenario assumptions for a region shown by the filled-out area of the bottom-right map. The downscaling technique is CCA. The cubic trend is derived from the statistical model with the highest correlation between statistically modeled and observed precipitation.

Source: Adapted from Hertig and Jacobeit (2008).

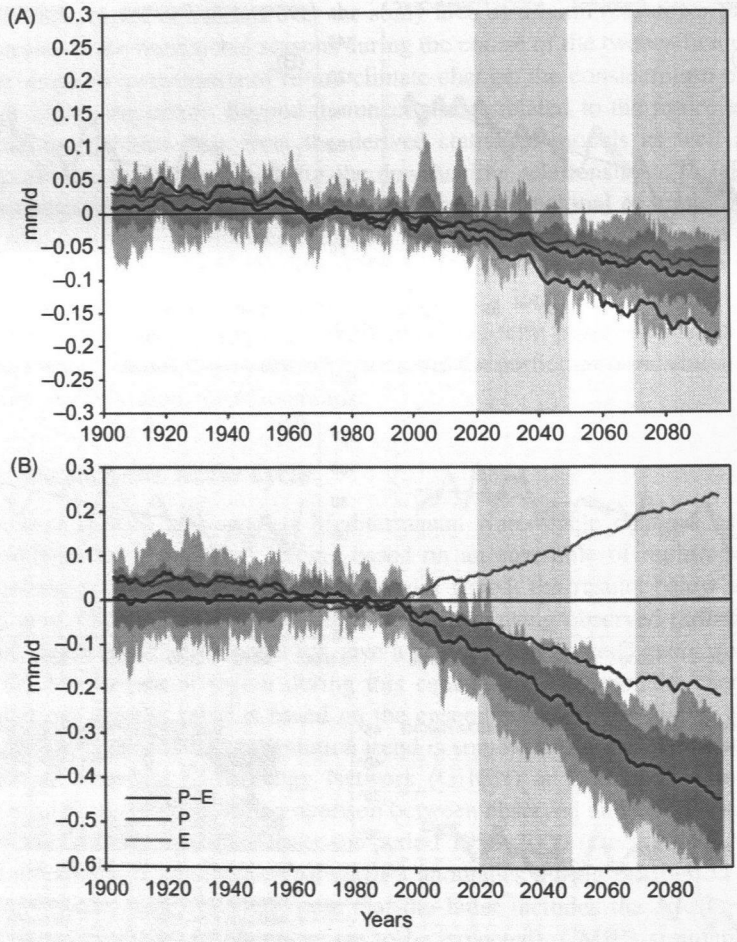

Figure 8.5 Mediterranean water-cycle anomalies over the period 1900–2100 relative to 1950–2000. Area-averaged evaporation (brown), precipitation (blue), and precipitation minus evaporation (black; P−E) are based on an average of CMIP3 model runs. For P−E, the envelope of individual model anomalies and the 1 standard deviation interval around the ensemble mean are also shown (light gray and dark gray shading, respectively). Data are 6-year running means of annual mean area-averages over an area broadly defining the Mediterranean region: (A) land only; (B) sea only. Focus periods are highlighted in yellow. (For interpretation of the references to color in this figure legend, the reader is referred to the web version of this book.)
Source: Adapted from Mariotti et al. (2008).

The amplitude of the mean precipitation anomaly foreseen by 2020–2049 (~0.1 mm/day or 36 mm/yr) is comparable to that of the driest decadal spells experienced by the Mediterranean region during the twentieth century. Since the multi-model ensemble average has internal variability with reduced amplitude, actual

variability would be larger than that depicted by the ensemble mean. As precipitation is the main driver of the land-surface hydrological cycle, other major hydrological indicators would also change correspondingly. Soil moisture would decrease progressively, as would runoff and river discharge, reducing the water available for irrigation and other uses. Evapotranspiration would also decrease because of the drier land surface, but, as increased surface temperature favors higher evaporation, the rate would be half that of precipitation. By 2070–2099, the projected effective precipitation (P − E) decrease over land is about 0.09 mm/day (0.01 mm/day per decade or 3.6 mm/yr per decade).

While the "forced" drying found by Mariotti et al. (2008) over land is large, projected changes for the Mediterranean Sea are even more dramatic. Unlike the surrounding land region, where evaporation decreases, the projected precipitation reduction over the sea is accompanied by a roughly equally strong increase in evaporation due to increased SST (ultimately due to more energy input from greenhouse warming). As a result, a 0.4 mm/day (or 146 mm/yr) increase in the loss of freshwater (E − P) at the sea surface is projected toward the end of the twenty-first century. This change is large, roughly equal to what is typically received in total by the Mediterranean Sea on an annual basis as discharge from neighboring land and as inflow from the Black Sea (Mariotti et al., 2002). Currently, a main freshwater source to the southeastern Mediterranean, the Black Sea inflow may also change, as it would receive less freshwater at the surface. As a result, the freshwater deficit that already characterizes the Mediterranean Sea would significantly increase according to these projections, with a cumulative freshwater deficit by 2100 of $1.54 \times 10^8 m^3$ (trend is −0.045 mm/day per decade or −16 mm/yr per decade). This would be further exacerbated by the decrease in river discharge from surrounding regions (cumulative decrease is $2.54 \times 10^7 m^3$). As in the past, these changes, if they materialize, can have important implications for the Mediterranean Sea (Rohling and Hilgen, 1991). Overall, the increase in the sea's freshwater deficit would contribute to increase salinity. The degree of the salinity increase would also depend on the strength of the freshwater input from the Atlantic Ocean at the Gibraltar Strait (see Section 8.4).

Climate-change projections typically suffer from major intermodel discrepancies, with models often not even agreeing on the direction of change (IPCC, 2007). In contrast, a qualitative model consistency regarding "forced" twenty-first-century Mediterranean water-cycle changes is among the highest globally (quantitative intermodel differences exist; see below for a discussion on caveats and uncertainties associated with these projections). Based on Mariotti et al. (2008), most models in this ensemble show a decrease in P − E already by 2020–2049, and in all by 2070–2099 (Figure 8.5).

By 2070–2099, all models in this ensemble show a decrease in precipitation and an increase in evaporation over the Mediterranean (a high degree of intermodel consistency of Mediterranean precipitation projections was also reported in IPCC, 2007); most models under consideration show a more moderate decrease in evaporation on land. The increase in the projected forced freshwater deficit over the Mediterranean is estimated at between −0.25 and −0.55 mm/day (or −91 and 200 mm/yr, respectively). Uncoupled RCM simulations in the framework of

the ENSEMBLES project also provide broadly similar results (Sanchez-Gomez et al., 2009). A suite of fully coupled RCM simulations from the CIRCE project allows the evaluation of the impact of coupled processes on these projections (see Section 8.4.2).

The projected twenty-first-century Mediterranean water-cycle changes described above would result from a general increase in moisture divergence across the subtropical dry zones, a consequence of mean climatological moisture divergence and rising humidity; the northward expansion of the Atlantic Hadley Cell (Held and Soden, 2006; Lu et al., 2007; Seager et al., 2007), and, to a large extent, a positive trend of the northern hemisphere Annular Mode (Previdi and Liepert, 2007). Projected water-cycle changes could have substantial consequences for the Mediterranean region. For land areas, soil moisture and river discharge decreases could impact water resources, ecosystems (e.g., natural vegetation cover, as discussed in Anav and Mariotti, 2011), and socioeconomic activities. It may be speculated that increases in Mediterranean Sea surface freshwater deficit could potentially increase salinity and impact circulation and sea level.

Although there is a high degree of intermodel consistency among the CMIP3 models regarding Mediterranean climate projections, uncertainties need to be carefully evaluated. These include general uncertainties associated with CMIP3 projections due to model errors (e.g., limited model resolution or the parameterization of physical processes), the effects of "internal" variability (from purely atmospheric modes or modes of coupled interactions within the ocean–atmosphere–land system), and uncertainties in future emission paths and natural radiative forcings (e.g., future volcanic eruptions). The uncertainty in emission paths is likely to play a larger role later in the twenty-first century, when differences among scenarios become larger. In addition to the above-mentioned general uncertainties, there are also region-specific uncertainties, including potential errors and limitations in the CMIP3 models' representation of regional climate variability, Mediterranean Sea circulation, and regional climate feedbacks (see also Section 8.5).

The role of "internal" variability on future water-cycle variations can be best understood by looking at past regional water-cycle variability and comparing this with the results from the CMIP3 twentieth-century simulations. Observational analyses of twentieth-century water-cycle variability in this region show long-term trends, including a tendency for increased surface aridity and increased Mediterranean Sea evaporation. These changes are not inconsistent with the "forced" changes depicted by the CMIP3 simulations as a result of increases in greenhouse-gas concentrations during this century. However, observational precipitation and evaporation records also include decadal variations that have a much larger amplitude than the above-mentioned simulated long-term trends (e.g., for precipitation, observed decadal anomalies are about two orders of magnitude larger than the simulated trend). As much as both observational errors and model errors can contribute to this discrepancy, this also highlights the important role of internal variability in determining observed decadal anomalies. One investigation, also based on CMIP3 projections, suggests that in the Mediterranean, "forced" changes are likely to become distinguishable from the "noise" created by internal decadal variations in decades beyond

2020–2030 (Giorgi and Bi, 2009). Hence, at least in the short term (roughly, 10–30 years), regional decadal anomalies and any potential for decadal predictability are likely to be critically dependant on the regional impacts of decadal modes of variability "internal" to the climate system.

The development of next-generation climate projections in the framework of CMIP5 (Coupled Model Intercomparison Project, phase 5; Taylor et al., 2009) will allow further evaluation of the uncertainties in regional climate outlooks. The analysis of these projections for the Mediterranean should be accompanied by efforts to better understand the role and predictive potentials of internal climate variability for regional decadal predictability and by continuing efforts to monitor Mediterranean water-cycle characteristics so as to be able to detect future long-term changes early on.

8.3.3 Climate Extremes

The European heat wave of summer 2003 has received considerable attention because of its potential link to both the larger-scale warming patterns (e.g., global warming) and the large non-harvest-related loss of life associated with it (Fouillet et al., 2006; Zaitchik et al., 2006). Several studies found that this regional heat wave was unique in comparison with the instrumental climate record. In fact, it has been suggested that such an extreme event could be explained by an increased variability, which in turns made heat waves more likely, ruling out the hypothesis that heat waves like the one in Europe in 2003 can occur by chance (Schär et al., 2004). Understanding and quantifying how anthropogenic climate change is affecting the intensity and frequency of extreme events has become a priority in climate studies (Kharin and Zwiers, 2000, 2005; Meehl et al., 2000; McGuffie et al., 1999; Vitolo et al., 2009).

The 2003 heat wave represents the archetype of an extreme event that, recently, has been widely analyzed in the Mediterranean, where the impact of global warming on human activities and natural ecosystems is of major concern (Rosenzweig et al., 2007; Bleu, 2009). Some EU projects (PRUDENCE, ENSEMBLES) have made available a large number of RCM scenario simulations facilitating statistical analysis of extremes in surface fields (temperature, rainfall, wind) with more robust estimates (Fowler et al., 2007, Coppola et al., 2010). Using an ensemble of RCMs (Baettig et al., 2007; Beniston et al., 2007; Frei et al., 2006) or single RCMs (Gao et al., 2006; Goubanova and Li, 2007; Sanchez et al., 2004; Semmler and Jacob, 2004), a general increase in temperature, rainfall, and drought extremes is projected for the end of the twenty-first century in A2 and B1 scenarios. An increase in the extremes of cyclone intensity over the Mediterranean Sea, clearly associated with the formation of tropical cyclones, has also been simulated (Gaertner et al., 2007). However, the robustness of these results, in terms of changes of rainfall distribution extreme tails, for the Mediterranean region has been questioned by Boberg et al. (2009) and Buonomo et al. (2007). In addition to the changes in CO_2 content in the atmosphere, which is not the only anthropogenic parameter affecting the extremes in the future, an afforestation–deforestation study has highlighted the relevance of the land-use change in determining surface extremes (Anav et al., 2010).

In order to examine changes in extreme statistics of near-surface climate parameters, such as the heat waves, long simulations of the present and future Mediterranean climate conditions are needed. An alternative approach to the studies mentioned in the previous paragraph is using a grand ensemble of climate simulations. The term *grand ensemble* is borrowed from statistical mechanics and is used to indicate a perturbed physics (parameter values), perturbed boundary conditions, and perturbed initial condition ensemble. Here, we apply extremes value theory to simulation results from the climateprediction.net (CPDN) project that is the first distributed computing climate project of its kind (Allen, 1999). In particular, we refer to the first distributed computing experiment, known as the "slab-model experiment." The initial ensemble was composed, at the time of writing of this study, of roughly 54,000 individual climate-change experiments, reduced to roughly 50,700 after quality control. Each experiment is comprised of three slab-model simulations. This data set is an expanded version of the one used by Piani et al. (2005) and described therein. Individual experiments are composed of three separate 15-year climate simulations conducted with the slab version of the United Kingdom Meteorological Office Unified Model described in detail by Pope et al. (2000). The first of the three simulations is done to calibrate the model. The second is a control run, with preindustrial levels of CO_2 concentrations. The last is a $2 \times CO_2$ simulation. For all the available simulations, we extract the last 5 years of the 15-year runs (preindustrial and $2 \times CO_2$ conditions) in order to have stationary time series. We collect all selected 5-year intervals. Considering more than 50,000 simulations, we have a very large number of intervals, enough to avoid small-sample instability of the statistical analysis. Maxima (minima) of daily maximum (minimum) temperature are extracted from each 5-year interval. This process is performed for the Mediterranean region as defined by Giorgi (2002).

Here, we analyze the probability density function (PDF) of all the time series and of the extreme's time series. An efficient method for displaying a statistical data summary is a box plot graph. The box plot in Figure 8.6 summarizes the following statistical measures: median, upper, and lower quartiles, and the minimum and maximum data values.

The box itself contains the middle 50% of the data. The upper edge (hinge) of the box indicates the 75th percentile of the data set, and the lower hinge indicates the 25th percentile. The range of the middle two quartiles is known as the interquartile range. The line in the box indicates the median value of the data. If the median line within the box is not equidistant from the hinges, then the data are skewed. The ends of the vertical lines, or "whiskers," indicate the minimum and maximum data values, unless outliers are present. In this case, the whiskers extend to a maximum of 1.5 times the interquartile range. The points outside the ends of the whiskers are outliers or suspected outliers.

The box plots of all time series (Figure 8.6A) show a significant shift of the bulk of the PDF in the case of future climate ($2 \times CO_2$) with respect to present-day climate data ($1 \times CO_2$). Both, the minima and maxima show a shift of about 3°C. The scenario box plots show a large number of outliers representing a change in the tails of the distribution. A rough idea of the behavior of the tails could be

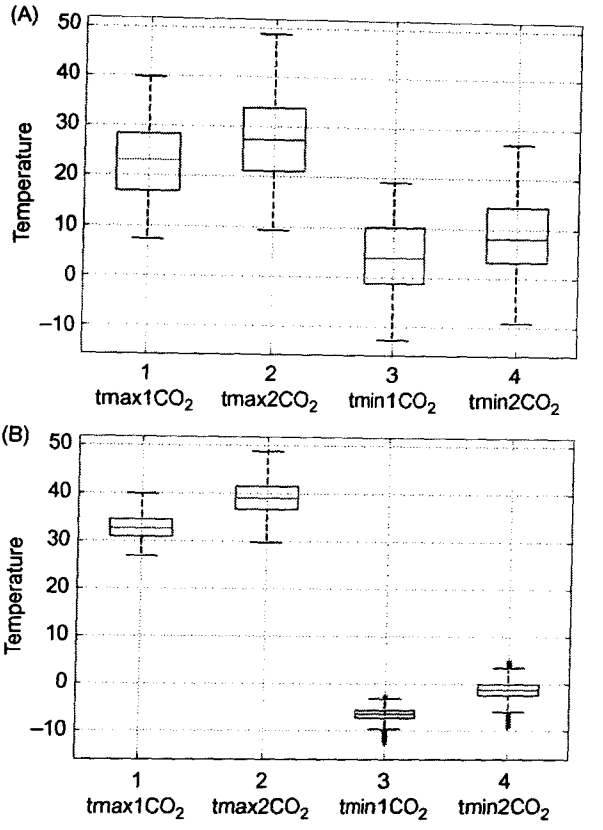

Figure 8.6 Box plot graph for the maximum (1 and 2 in abscissa) and minimum (3 and 4 in abscissa) temperatures, both in the present climate ($1CO_2$, 1 and 3) and scenario ($2CO_2$, 2 and 4) runs over the Mediterranean region. (A) All time series. (B) The extremes for block lengths of 5 years.

obtained by analyzing the box plot of the extremes (minima and maxima) for a specific block length. The distribution of temperature extremes computed over a 5-year interval is shown in the bottom panel of Figure 8.6. The main point rising from a visual inspection is not only the shift of the extremes PDF to higher values but also its broadening.

The statistical downscaling approach of Hertig and Jacobeit (2008) also allows for the investigation of the impact of climate change on temperature extremes (Hertig et al., 2010). In Figure 8.7, we report statistical assessments of changes of the 5th percentile of minimum temperatures in winter and of the 95th percentile of maximum temperatures in summer, comparing the period 2071–2100 under A1B scenario conditions with the reference period 1961–1990. Minimum temperature changes in winter are related to the question of whether the frost hazard risk will be modified under future climate change, whereas maximum temperature

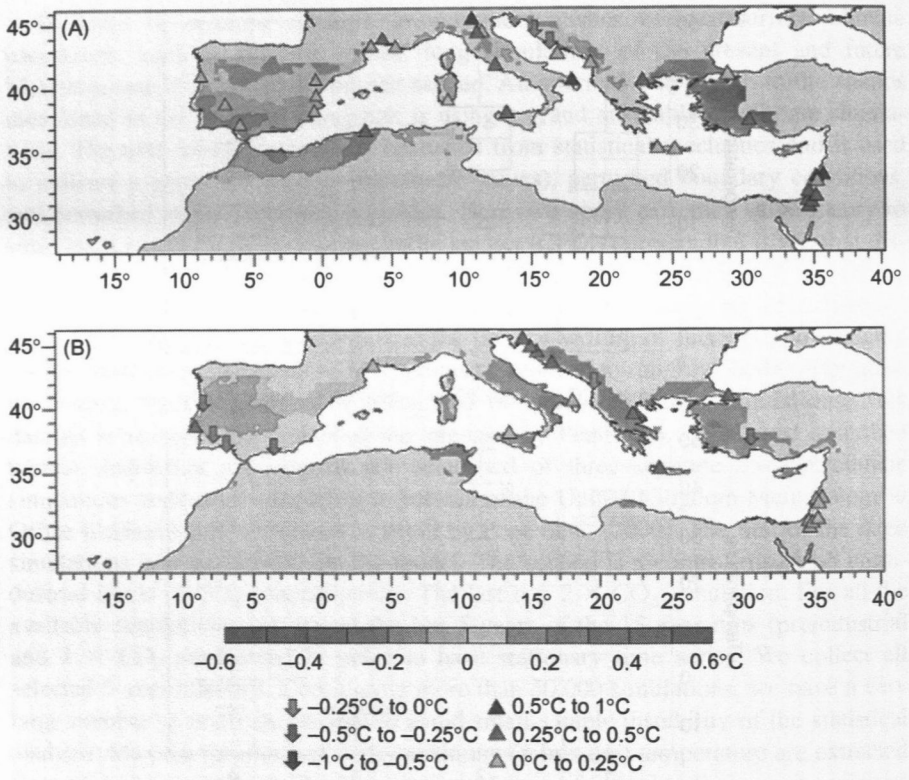

Figure 8.7 Changes of the (A) 5th percentile of minimum temperatures in winter (December–February) and 95th percentile of maximum temperatures in summer (June–August) (B) according to statistical downscaling assessments using ECHAM5/MPI-OM predictors (1000 hPa/500 hPa thickness and 500 hPa geopotential heights) under SRES A1B scenario assumptions; differences of the seasonal extremes indexes between the periods 2071–2100 and 1961–1990 in °C. Statistical downscaling techniques include multiple-regression analysis in the case of station-based assessments (local symbols) and CCA for grid-based assessments (colored areas). (For interpretation of the references to color in this figure legend, the reader is referred to the web version of this book.)

changes in summer refer to the question whether of the hottest days will get even hotter. The downscaling assessments are based on station data as well as on highly resolved gridded temperature data for the Mediterranean area. As large-scale predictors, 500 hPa geopotential heights (representing the atmospheric circulation) as well as 1000 hPa/500 hPa thickness fields (representing tropospheric temperatures) have been considered.

Obviously there are mainly increases of both extremes indexes (see red areas in Figure 8.7). The station-based assessments indicate that there will be widespread increases of the 5th percentile of minimum temperatures in winter, with the largest

warming rates up to 1°C in the eastern Mediterranean area as well as in the central-northern Mediterranean region (Figure 8.7A). This general result is largely confirmed by the grid-based assessments, but some regions also show slight decreases of extreme minimum temperatures in winter, most pronounced for the southern parts of the Iberian Peninsula and the western parts of Mediterranean North Africa. For the 95th percentile of maximum temperatures in summer (Figure 8.7B), both station-based and grid-based assessments project increases in the central and eastern Mediterranean area, with values up to about 0.5°C, but slight decreases over parts of the Iberian Peninsula. Comparing the results for winter and summer, we partly get an indication that the intraannual extreme temperature range will decrease until the end of twenty-first century under enhanced greenhouse warming conditions—mainly in the eastern Mediterranean area—because extreme minimum temperatures in winter will experience greater increases as compared with extreme maximum temperatures in summer. For other areas in the central-northern and western Mediterranean region, a mixed picture arises regarding changes of extreme temperatures for parts of the Iberian Peninsula, possibly even including slight decreases of the corresponding percentiles. In general, however, the results indicate that changes in temperature extremes do not follow a simple shift of the whole temperature distribution to higher values, implying nonsymmetric changes in the frequency distributions of Mediterranean temperatures.

Precipitation extremes have also been analyzed over the Mediterranean region of France using a high-resolution ARCM. Three simulations were carried out over the twenty-first century, following the IPCC scenarios B1, A1B, and A2, using the RCM ALADIN-Climate at a 12-km resolution on a domain centered over France. The RCM was constrained at its lateral boundary by corresponding global projection results performed with ARPEGE-Climat. The domain of integration is relatively small because of the heavy computational cost of the high resolution, but this limitation is not detrimental to the representation of intense precipitation, whereas the increase of resolution significantly improves the representation of these extremes.

All the climate scenarios show a decrease of the mean precipitation in the Mediterranean region of our domain between the beginning and the end of the period, except during winter (DJF) in the A2 scenario (not shown). However, over this Mediterranean region, the heaviest rainfalls tend to be stronger. The quantile–quantile diagrams of Figure 8.8 illustrate this finding. They represent the change of the daily precipitation's spectrum averaged over a Mediterranean box (see Figure 8.9A) during autumn (SON). Each of the three curves on the two plots reproduces the values of the quantiles in the distribution of daily precipitation simulated over the period 2070–2100 with one of the three IPCC scenarios, versus the values of the same quantiles in the daily precipitation distribution simulated in the control simulation over the 1970–2000 period. It appears on these plots that the precipitation decreases in the future—especially in the A2 scenario—under the threshold of 30 mm/day but increases in the tail of the distribution in the A1B and A2 scenarios. This result reflects a broadening of the precipitation distribution with climate change and thus an increase of the proportion of total rainfall from heavy falls.

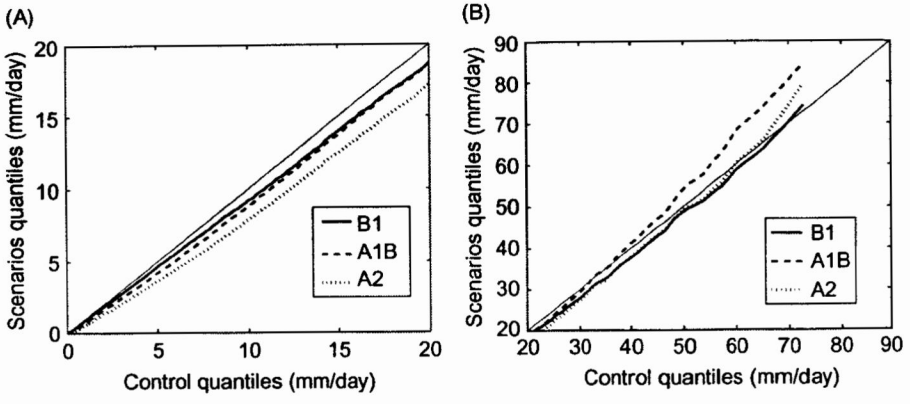

Figure 8.8 Quantile–quantile plots—control simulation versus scenarios—of daily precipitation quantiles (mm/day) in autumn (SON). Quantiles are averaged over the box shown in the top left map. (A) Quantiles from 0 to 20 mm/day. (B) Quantiles from 20 to 90 mm/day. Quantiles (from 0.1% to 99.9%) of the control simulation, in the period 1970–2000, are sorted along the x-axis, quantiles of the scenarios over the period 2070–2100 are sorted along the y-axis. Solid line: B1; dashed line: A1B; dotted line: A2.

Figures 8.9 and 8.10 offer a global view of the "inverse" behavior of the mean and of the higher extremes. For each grid point we consider, there is an inversion in the sign of the precipitation's evolution when the following conditions are satisfied: (1) The mean difference in precipitation between 2070–2100 and 1970–2000 is negative (decrease of precipitation in the future). (2) There is a quantile of precipitation exceeding 2 mm/day over which the mean difference of precipitation between the same periods is positive (increase of the heavy rainfall), and under which it is negative. Figure 8.9A–C indicates for the autumn season (SON) the order of this inversion quantile, if there is any, and Figure 8.9D–F its value. Mean differences of autumn precipitation between 2070–2100 and 1970–2000 are drawn on Figure 8.10A–C, and the corresponding mean relative differences (in %) of precipitation exceeding the inversion quantile are shown on Figure 8.10D–F.

These maps show that an inversion, as defined above, occurs over a large extent of the Mediterranean region in all three scenarios, particularly in A1B and A2. The order of the inversion quantile is generally quite high: it ranges from 96% to 99.9%, which correspond to amounts of precipitation between 30 and 100 mm/day. They are higher in the A2 scenario, which is the one leading to the most enhanced drying in terms of mean precipitation. However, the increase of the precipitation exceeding the inversion quantile remains moderate. They are mainly between +5% and +10%, except in some mountainous areas (Alps and Cévennes), where they reach +20%. The same features can be found in spring (MAM) and summer (JJA), although they are weaker, and no distinct pattern was detected in winter (DJF) regarding the extremes of precipitation. Considering the high values of the inversion quantile's

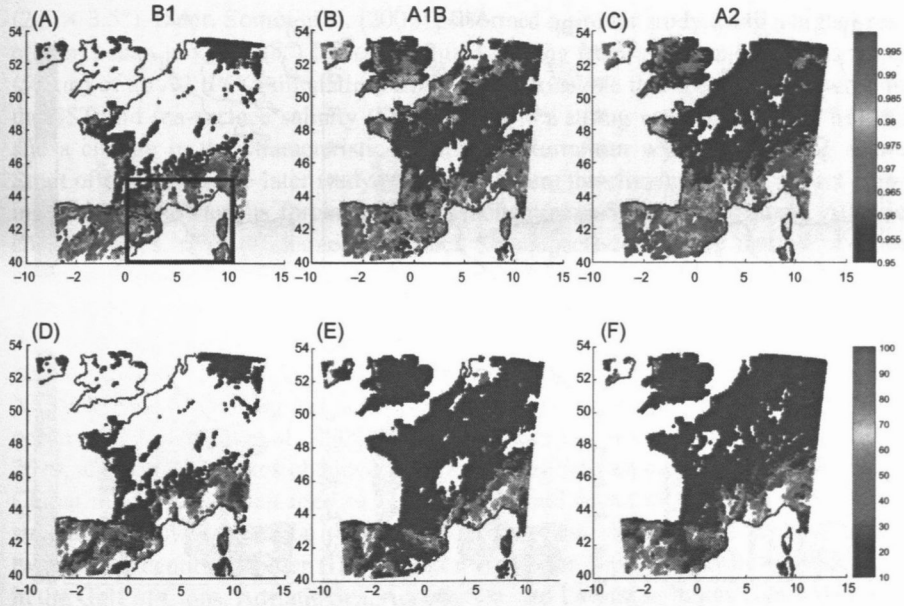

Figure 8.9 Inversion quantiles of autumn (SON) daily precipitation between 1970–2000 and 2070–2100 (colored areas). (A, B, and C) Order of the quantile (0.95 means the 95th centile) for B1, A1B, and A2 scenarios, respectively. (D, E, and F) Value of the inversion quantile (mm/day) for B1, A1B, and A2 scenarios, respectively. See text for details. (For interpretation of the references to color in this figure legend, the reader is referred to the web version of this book.)

orders and the rather small differences in the precipitation over this relative threshold, it would be suitable to complete this work with an appropriate testing of the statistical significance of the results.

8.4 Future Projections for the Mediterranean Sea

8.4.1 *Temperature, Salinity, and Ocean Circulation*

Many studies have been published about the Mediterranean regional climate change dealing with mean state changes, variability, seasonality, or extreme events. From these studies and from an oceanographic point of view, we conclude that the Mediterranean climate would become warmer and drier in the twenty-first century. This could have an impact on the salinity and temperature of the surface-water masses and on their density and surface circulation. The influence on the density is then unknown (saltier and warmer waters) as well as on the deep-water formation process and the Mediterranean outflow water that enters the Atlantic Ocean after overflowing at the Strait of Gibraltar. However, until recently, in the context of the CIRCE project, very few studies were focused on the Mediterranean Sea and its

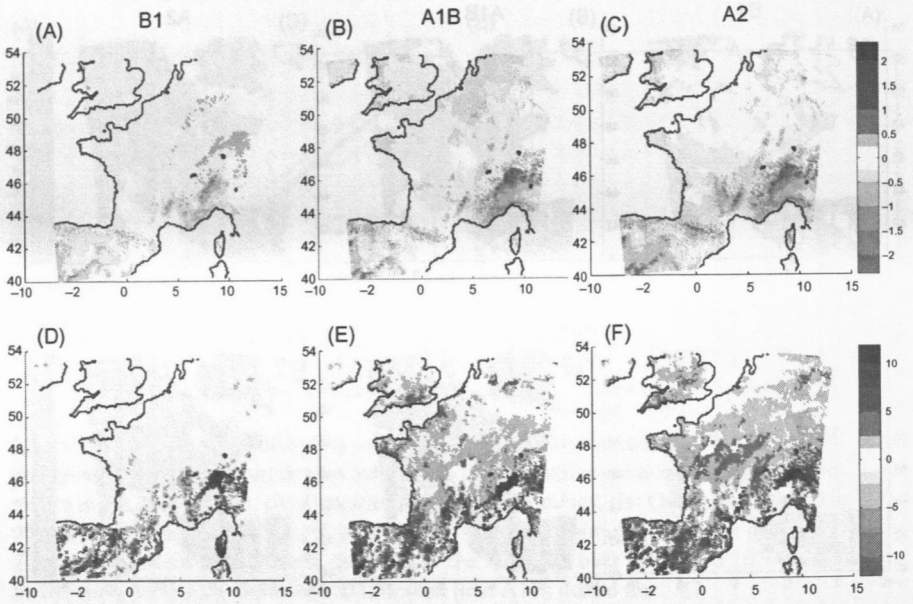

Figure 8.10 Difference of autumn (SON) daily precipitation between 1970–2000 and 2070–2100. (A, B, and C) Mean difference of daily precipitation (mm/day) for B1, A1B, and A2 scenarios, respectively. (D, E, and F) Relative difference (%) of daily precipitation exceeding the "inversion" quantile of Figure 8.9.

possible evolution in the twenty-first century, and none of them were coordinated efforts to tackle the uncertainty issue.

Concerning the methodology, these studies generally underlined some key points when constructing climate-change scenarios of the Mediterranean Sea: (1) taking into account the various Mediterranean Sea forcings, such as heat, water and momentum fluxes, river discharge, Black Sea inputs, and near-Atlantic Ocean characteristics; (2) performing a control or present climate simulation long enough to reach the stability of the ocean model; (3) reaching a realistic present climate state of the Mediterranean thermohaline circulation (MTHC) representing the various water masses and their interactions; and (4) performing transient climate simulations in order to solve the problem of the initial conditions under future climate conditions.

Recently, CMIP3 GCMs were used to access the uncertainty range of the response of the Mediterranean water temperature, salinity, and sea-level change in the twenty-first century (M. Marcos, personal communication). This study mainly demonstrated that, because of their too-low spatial resolution, the GCMs are not able to simulate a realistic Mediterranean Sea in present climate and that their climate-change results are consequently doubtful.

A pioneer work using a high-resolution Mediterranean model was done by Thorpe and Bigg (2000) simulating a transient $2 \times CO_2$ scenario with a 1/4°-resolution ocean model forced by the air–sea fluxes of a low-resolution IPCC model

(2.5 × 3.5°). Later, Somot et al. (2006) performed a similar study using a higher-resolution ocean model (1/8°) forced by fluxes coming from a dynamical downscaling (50 km) of an A2 IPCC simulation. Both studies conclude that there is an increase in the SST and sea-surface salinity (SSS) leading to a strong weakening of the MTHC and a change in the characteristics of the Mediterranean waters outflowing at the Strait of Gibraltar. The later study took into account the climate-change impact coming from all the various forcings of the Mediterranean Sea (air–sea fluxes, Atlantic characteristics, river discharge, and Black Sea impact) concluding that all of them could be important contributors to the possible evolution of the sea characteristics.

Another example using a Mediterranean Sea model constrained with the outputs of a high-resolution atmosphere-only climate-change scenario, consists of an ocean climate-change scenario (SRES A2) simulation performed by means of the NEMOMED8 Mediterranean Sea model, a regional adaptation of the NEMO global ocean model (Sevault et al., 2009). In order to carry out this experiment from 1960 to 2099, atmospheric fluxes obtained from the resolution-varying version of ARPEGE-Climat model have been used to force the regional ocean model. Results from the simulation show convection processes becoming less important by the end of the twenty-first century. Winter (DJF) mean mixed-layer depth diminishes significantly in the Gulf of Lions, Adriatic Sea, Aegean Sea, and Levantine basin. This decrease is reasserted by the reduction of the yearly maximum mixed-layer depth estimated for the main Mediterranean deep-water formation areas, particularly in the Gulf of Lions (Figure 8.11).

Under this SRES A2 emission scenario, a general increase of temperature and salinity over the Mediterranean Sea is obtained from 2000 to 2099, both at the sea surface and in the deeper layers. Salinity presents an increment of +0.06 psu per decade at the sea surface and +0.035 psu per decade in the deeper layers during the twenty-first century. Concerning temperature, an average increase of 0.108°C per decade is deduced for the total water column, being more pronounced in the surface layer up to 150 m, in agreement with estimated SST trends of +0.26°C per decade.

According to the results of this simulation, the net water transport at the Strait of Gibraltar would vary from +0.05 Sv for the present climate results up to +0.07 Sv in 2099, basically due to a rise in water inflow during this period. This increment balances the increase of evaporated water simulated over the Mediterranean basin at the same time. In addition, the simulation presents a mean intensification of the Mediterranean circulation as well as a slight change of its pattern.

For the first time, Somot et al. (2008) used an AORCM coupling the regional atmosphere model and the regional ocean model of the Somot et al. (2006) study. A 140-year scenario was carried out using this model (SRES A2, 1960–2099) along with a twin control simulation (same length, no climate-change signal) repeating the 1960–1980 forcing. The results from this simulation can be directly compared with those of the SRES A2 climate-change simulation performed by Somot et al. (2006), since they used exactly the same Mediterranean Sea model and since the forcing of the stand-alone ocean simulation comes from the coupled one. Some results of this comparison are reported in Table 8.1, where the corresponding results of Thorpe and Bigg (2000) have also been included. The results of the coupled and

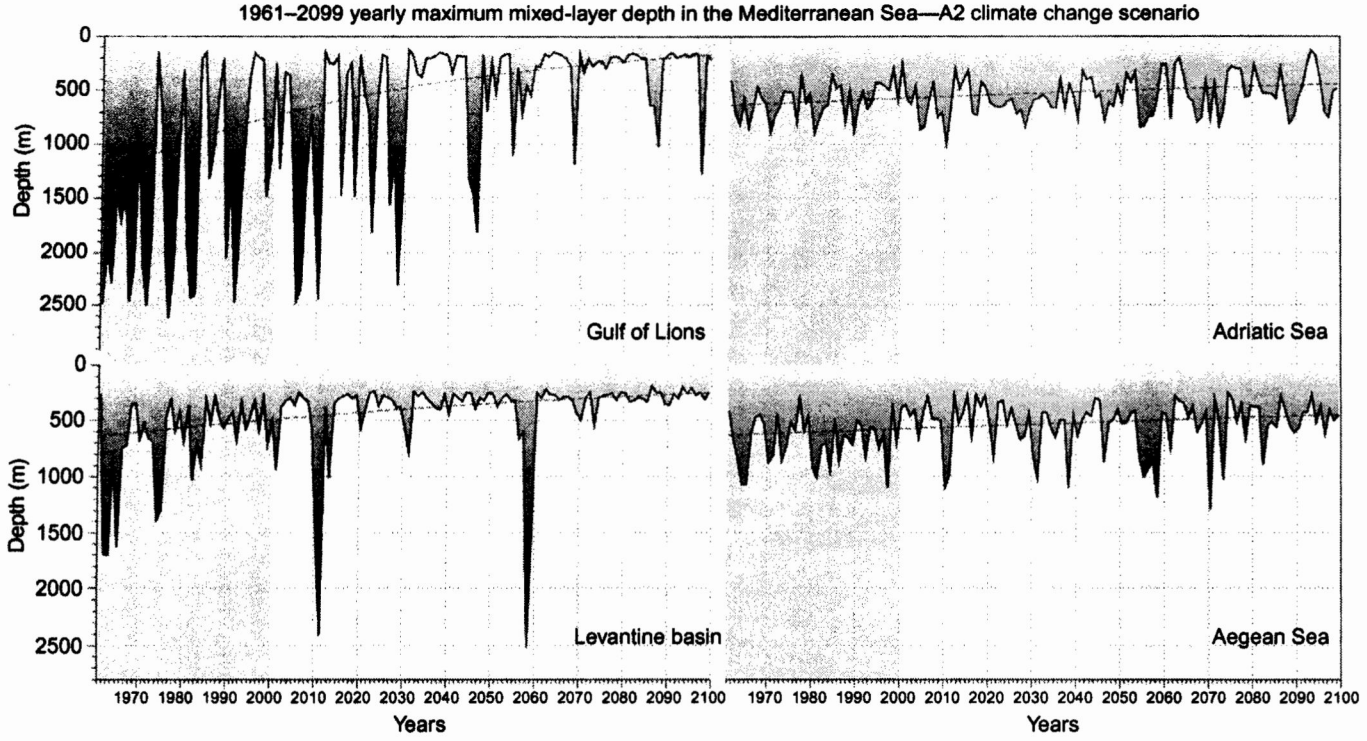

Figure 8.11 Time series of yearly maximum mixed-layer depth between 1961 and 2099, obtained from NEMOMED8 ocean-model simulation, under SRES A2 climate-change scenario conditions. The dotted line represents the exponential fit for the different time series.

Table 8.1 Mediterranean Sea Spatial Averaged Changes at the End of the Twenty-First Century as Compared with the Present Climate

	Thorpe and Bigg (2000)	**Somot et al. (2006)**	**Somot et al. (2008)**
Heat loss (W/m^2)/ water loss (mm/ day)/wind	Decrease/increase/ decrease	+4.4/+0.4/decrease	+2.7/+0.4/decrease
Mediterranean Sea SST/SSS	+4°C/-	+2.5°C/+0.33 psu	+2.6°C/+0.43 psu
MTHC	Strong weakening, warming and saltening of the deep layers	Strong weakening, warming and saltening of the deep layers	Slight weakening, warming and saltening of the deep layers
Strait of Gibraltar water transport	No change (1 Sv)	Almost no change (−4%)	Almost no change (−2%)
Mediterranean outflow water	Saltening (+0.12 psu), warming (+0.8°C), shallowing (from 1400 to 600 m)	Saltening (+0.45 psu), warming (+2.5°C), no change in density	Saltening (+0.36 psu), warming (1.8°C), lightening ($-0.1\,kg/m^3$)

The comparison is among the three studies published as of this writing.

associated uncoupled simulations are very similar as far as the SST is concerned. However, the MTHC remained stable in this coupled simulation, illustrating either the role of the coupling or the role of the MTHC present climate state in such a scenario simulation of the Mediterranean Sea. The warming and salinification of the Mediterranean Sea that is projected by the Somot et al. (2006) model is dominated by the increase in temperature, which in turn leads to an increasingly more stable water column. There is very little warming or salinification at levels below 2000 m. In the coupled simulation, the changes are dominated by changes in the Adriatic Sea and the increased formation of intermediate waters there (Tsimplis et al., 2008). Similar characteristics and changes of temperature and salinity have been found in the Mediterranean sections of global AOGCMs (Marcos and Tsimplis, 2008). However, these authors find that diffusion alone cannot account for the warming rates of the deeper waters; thus, some dense-water formation is still important for the models such as those in the regional coupled simulation. In addition, note that the reduction of dense-water formation is not, at least during the past decade, supported by observations either in the western Mediterranean or in the Adriatic Sea.

To go further in the analysis of this coupled simulation, we present here a discussion of some results of the oceanic component, those concerning the atmospheric component being discussed in Somot et al. (2008). In the AORCM simulation, the external forcing are the greenhouse gases and aerosols concentrations (SRES A2), the SST outside the Mediterranean area, and the Atlantic characteristics from the AOGCM CNRM-CM, and the rivers and Black Sea freshwater inputs coming from an ARCM simulation. This scenario is the first dedicated to the study of the Mediterranean Sea

for which no constraint is applied at the air–sea interface. This means that the low-level atmosphere variables, the air–sea fluxes, the SSTs, and the SSSs are completely free to adapt to the external forcing and are consistent with each other, contrary to the forced-mode scenarios (Thorpe and Bigg, 2000; Somot et al., 2006).

We first present the results spatially averaged over the entire Mediterranean Sea for the end of the twenty-first century (2070–2099 versus 1961–1990). The total surface heat-loss decreases by 2.7 W/m^2, explaining parts of the sea warming (the remaining part comes from the Atlantic Ocean); the total surface-water loss increases by 0.4 mm/day, leading to an increase in surface and volume-integrated salinity. The wind intensity slightly decreases, too. The SST increases (Figure 8.12) by 2.6°C, which is in very good agreement with Somot et al. (2006), showing that an uncoupled scenario can deliver the right value for the Mediterranean averaged SST change. However, the average SSS increase of 0.43 psu is a significantly larger value than that in Somot et al. (2006). As a result of these changes, the surface density decreases because the SST effect is slightly stronger than the SSS effect. In addition, the warming appears earlier (around 1980) than the SSS increase (around 2040) (see Figure 8.12). Consequently, the deep layers of the Mediterranean Sea warm and become saltier during the twenty-first century, with a slight weakening of the MTHC. At the Strait of Gibraltar, the net water transport does not change significantly, but the Mediterranean Overflow Water (MOW) layer that flows outside the Mediterranean Sea into the Atlantic becomes more salty (+0.36 psu), warmer (1.8°C), and lighter (–0.1 kg/m^3). This could affect the position and the characteristics of the Mediterranean Waters flowing into the Atlantic Ocean and consequently the Atlantic Meridional Overturning Circulation (AMOC). However, this effect

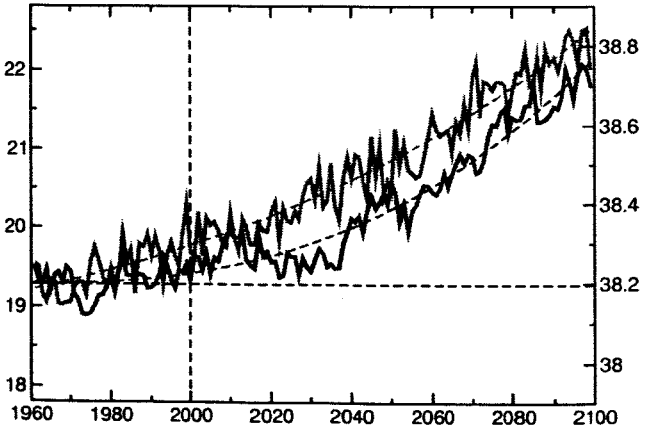

Figure 8.12 Yearly mean time series of the Mediterranean Sea average SST in red (in °C) and SSS in blue (in psu). The dashed lines are quadratic fits. Temperature and salinity curves are scaled by a factor of 5 so that their variations represent an equivalent density change. (For interpretation of the references to color in this figure legend, the reader is referred to the web version of this book.)

cannot be studied with the current model, as the Atlantic Ocean is considered as an external forcing only. Also note that the description of the Strait of Gibraltar is perhaps not adequate to well simulate how the Mediterranean changes propagate toward the Atlantic Ocean (see Sannino et al., 2009, on the issue of the resolution of the Strait of Gibraltar).

The spatial pattern of the warming and of the increase in salinity is very inhomogeneous in the coupled model at the end of the twenty-first century (Figure 8.13A and B). These patterns are driven by many ocean features represented only in a high-resolution ocean model. Few among them are as follows:

- The transport from the Atlantic: the Atlantic waters show warming and saltening minima.
- The change in the circulation: the Ionian Sea shows a strong change of its main jet that is deflected to the South, leading to a cyclonic anomaly in the circulation and a local maximum increase in SSS.
- The deep formation process: the Gulf of Lions area is an area of minimum warming, as the whole thermal inertia of the water column can play a damping role for the surface.
- The effect of the change of river discharge: the Adriatic and Aegean seas show a more pronounced increase in salinity than everywhere else as a consequence of a strong decrease in the Po and Black Sea freshwater inputs. This also leads to a local maximum increase in SST.

The seasonal cycle of the warming is relatively weak, with the maximum warming occurring in summer (range from +2.5 to +4°C) when the maximum climate warming also occurs over the land, and when the mixed-layer depth (and the ocean inertia) is the weakest. The minimum warming occurs in winter (+2 to +3°C) when the atmosphere also presents the minimum warming and the mixed layer is the deepest. Note that the maximum sea warming at the end of the twenty-first century (<+4°C) is from far lower than the climate warming in the surrounding land areas (Southeast Europe, >+6°C), increasing the land–sea contrast (Somot et al., 2008). This also underlines the negative feedback of the Mediterranean Sea thermal inertia and the positive feedback of the summer drying effect of the land.

In addition to SST and SSS, Figure 8.13 shows the warming and the saltening at a 100 m depth (Figure 8.13C and D) and at a 1000-m depth (Figure 8.13E and F). The 100 m depth signal still corresponds to the surface signal, with maximum values in the Aegean, the Adriatic, and the Ionian Sea. A deeper climate-change signal has been filtered, and it is mainly dominated by the water-mass formation process and the advection of the abnormal water masses. In our simulation, the 1000 m signal comes mainly from the Adriatic Sea, which is the only subbasin keeping an intense deep-water formation process and helping the ventilation of the deep layers through advection. Consequently, the maximum anomalies are driven by the Adriatic-originated waters that flow over the Otranto Strait and cascade at least up to 1000 m. These waters then invade the Ionian and Levantine basins in a cyclonic circulation attached to the bathymetry and invade the Tyrrhenian Sea after cascading over the Sicilian Strait. Part of the warmer and saltier waters even reached the Strait of Gibraltar before the end of the twenty-first century. At that depth and for the Mediterranean Sea, the convection–advection process seems to dominate the vertical diffusion to propagate the climate-change anomalies. It is worth noting that even the areas far from the main path of advection warm by at least 0.8°C at 1000 m.

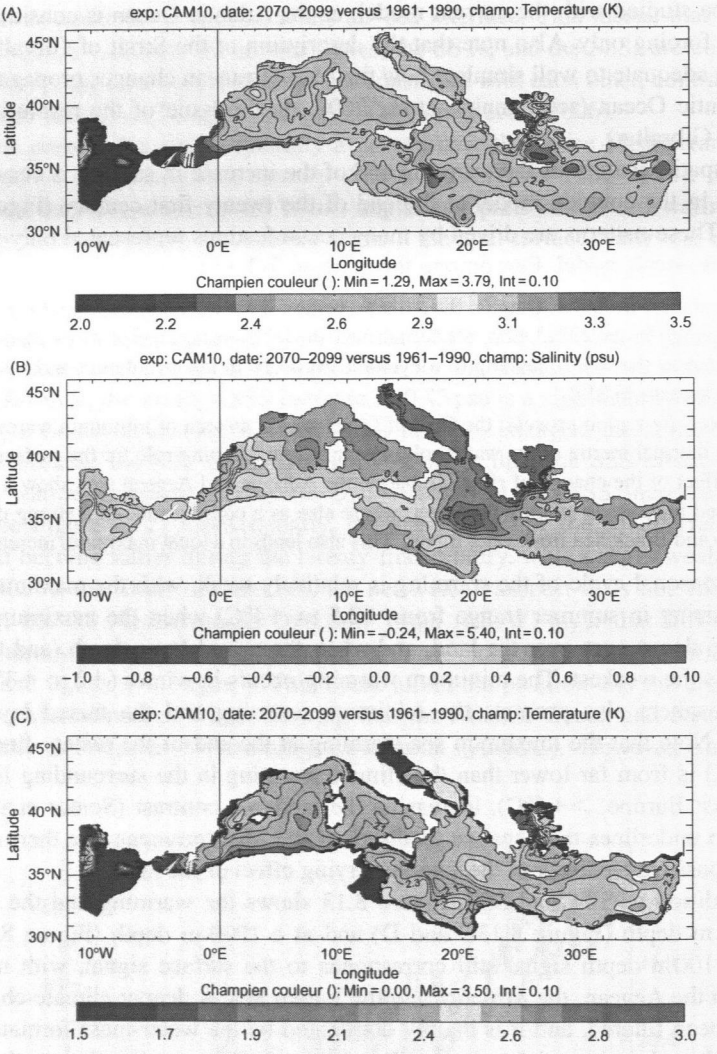

Figure 8.13 Differences in temperature (A, C, and E) and in salinity (B, D, and F) between the future climate (2070–2099) and the present climate (1961–1990) for the surface (A and B), at 100 m (C and D), and at 1000 m (E and F).

The Aegean maximum values of warming and saltening seem to be trapped in their basin of origin and do not export the signal toward the rest of the Mediterranean Sea. In the future, at least in this particular simulation, the Mediterranean Sea does not switch to a mode for which the Aegean Sea would become the main source of the eastern Mediterranean Sea deep water. This mode was already observed in the 1990s during the so-called eastern Mediterranean Transient (Roether et al., 1996), and its possible repetition in the future is a key issue for the scientific community.

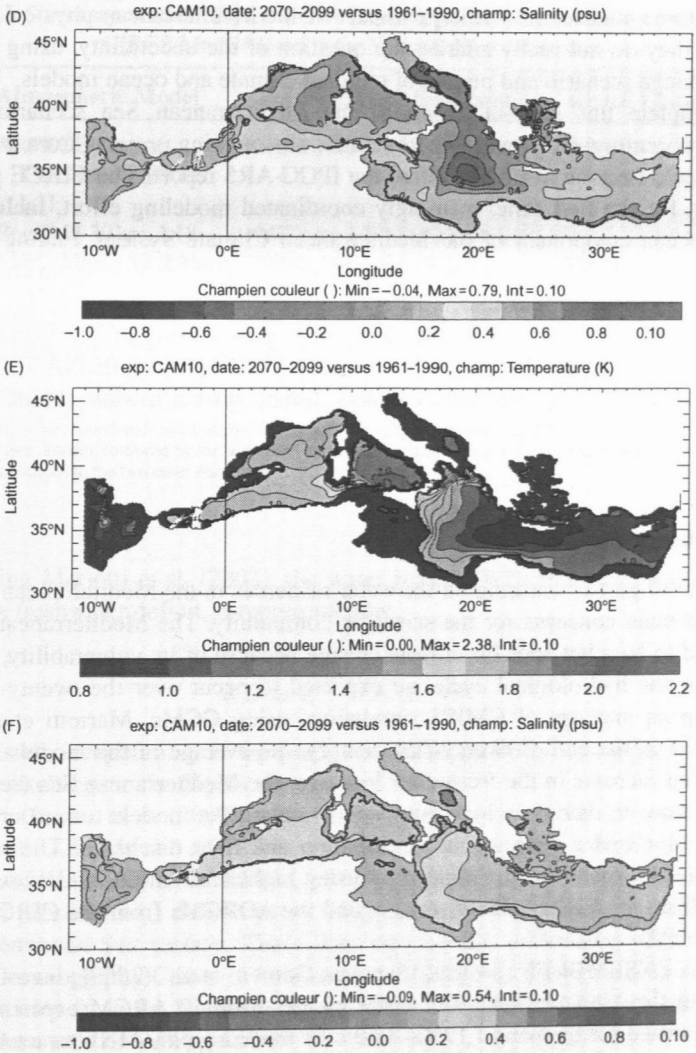

Figure 8.13 (Continued)

Based on these A2 simulations, some climate-change impact studies have also been published—on the Gulf of Lion cascading process (Herrmann et al., 2008), on the Gulf of Lion biogeochemistry (Herrmann, 2007), on the Mediterranean Sea-level change (Tsimplis et al., 2008), on the geographical habitat of Mediterranean endemic fishes species (Ben Rais Lasram et al., 2010), and on the wave-field response (Lionello et al., 2008). Except on the sea level and the waves for which the results show that the Mediterranean Sea is not a hot spot of the climate change,

the other three studies show a large impact of the Mediterranean physical changes. However, they do not really address the question of the uncertainty, using only one climate-change scenario and one set of regional climate and ocean models.

To complete this state-of-the-art of the Mediterranean Sea scenario for the twenty-first century, we would like to mention the ongoing projects from which new results should become available before the IPCC-AR5 report. The CIRCE project is proposing, for the first time, a strongly coordinated modeling effort, including the regional ocean component of the Mediterranean Climate System. Ending in 2011, it will allow access to the response of the Mediterranean Sea to climate change over the period 1950–2050 and under the A1B emission hypothesis using six different AORCMs. We should also mention other ongoing or starting efforts using regional ocean forced by air–sea fluxes (the European SESAME project, the VANIMEDAT-II project in Spain) or regional fully coupled climate system models (MedCORDEX, HyMeX).

8.4.2 Water Budget

The impact of global warming on the water resources in the Mediterranean region is one of the main concerns for the scientific community. The Mediterranean basin is considered to be a hot spot for climate change because of its vulnerability, so major changes in the hydrological cycle are expected to occur over the twenty-first century. From an analysis of CMIP3 simulations using GCMs, Mariotti et al. (2008) showed that at the end of twenty-first century, the average of the models simulates a significant increase in the freshwater loss over the Mediterranean Sea (see Section 8.3.2). Moreover, there is a high consistency among the models toward an increase in evaporation and a decrease in precipitation and river discharge. The robustness of these results has been investigated by using higher-resolution models such as the ARCMs from the ENSEMBLES project and the AORCMs from the CIRCE project (see Table 8.2).

In the ENSEMBLES project, Sanchez-Gomez et al. (2009) investigate the changes in the Mediterranean Sea water budget from 12 ARCM experiments that were performed for the period 1950–2050 over the European–Mediterranean domain at 25km horizontal resolution. Some experiments have been pursued until 2100 (seven models). Different GCMs SRES A1B scenario simulations have driven the ARCMs. The SST forcing the ARCMs are issued from the same GCMs experiments.

In addition, in the CIRCE project, the change of the water budget is determined from five AORCM experiments that were also performed for the period 1950–2050. In this case, the model's horizontal resolution is ~50km over the European–Mediterranean domain, with an interactive ocean model. Three of the AORCMs are coupled with a global ocean model, allowing for representation of the interaction and feedbacks of the Mediterranean Sea onto the large-scale circulation. For all the AORCMs, the transport through the Strait of Gibraltar, resulting from the nudging of the Mediterranean sea component in the near-Atlantic, is time dependent.

Table 8.2 Summary of the Different Model Components and Resolutions for Each of the CIRCE Models Used in the Water-Budget Analysis

	Atmospheric Model	Mediterranean Sea Model	Global Ocean Model
CNRM	ARPEGE-Climat TL159c2.5 (50 km), L31	NEMOMED8 1/8° (9–12 km), L43	OPA9 2° (0.5° equator), L31
ENEA	RegCM3 30 km, L18	MITgcm 1/8° (9–12 km), L42	
INGV	ECHAM5 T159 (80 km), L31	OPA9 1/16° (7 km), L71	OPA8.2 2° (0.5° equator), L31
MPI	REMO 25 km, L31	MPI-OM 1/8° (9–12 km), L30	
LMD	LMDz 30 km, L19	NEMOMED8 1/8° (9–12 km), L43	OPA9 2° (0.5°equator), L31

For each model, in the second and third column, the second line corresponds to the model horizontal resolution in the Mediterranean Sea domain, followed by the number of vertical levels (Ln). When a global ocean model is mentioned, this means that it is coupled to the two other components.

Following Mariotti et al. (2002), the water budget (WB) over the Mediterranean Sea, here a freshwater deficit, is represented by:

$$\mathrm{WB} \approx E - \mathrm{P} - \mathrm{R} - \mathrm{B}$$

where E is the evaporation, P the precipitation, R the river discharge, and B the Black Sea discharge in the Mediterranean Sea.

Sanchez-Gomez et al. (2009) performed a validation study for the period 1950–1999 for both ARCMs and AORCMs and also for GCMs from CMIP3 integrations. They showed that ARCMs, AORCMs, and GCMs underestimate the E − P (evaporation minus precipitation) difference as compared with observational data sets over the Mediterranean Sea surface. These data sets are the evaporation field from the National Oceanography Centre of Southampton (NOCS) data set (Josey et al., 1999), the precipitation from the Hamburg Ocean Atmosphere Parameters and Fluxes from Satellite Data set (HOAPS) (Andersson et al., 2007), and the river discharge presented by Ludwig et al. (2009) and the Black Sea freshwater discharge by Stanev et al. (2000). Sanchez-Gomez et al. (2011) performed an exhaustive analysis of Mediterranean water- and heat-budget estimates provided by state-of-the-art observational data sets in which the above-mentioned are included. The GCMs, though running with a coarse resolution, provide E − P values that are close to those of the regional models. The regional models clearly improve the representation of R and B with respect to GCMs, indicating that the finer resolution represents more accurately the river discharge, which depends on small-scale processes.

Table 8.3 shows the uncertainty intervals associated with the future changes in the Mediterranean water budget for both ARCMs and AORCMs and also for CMIP3 integrations. The values indicate the percentage of change represented by anomalies of two

Table 8.3 Percentages of Area-Averaged Mean Changes in the Mediterranean Sea for Evaporation (E), Precipitation (P), E − P, River Discharge (R), Black Sea Discharge (B), and Total Water Budget (WB) for the Periods 2020–2049 and 2070–2099 as Compared with 1950–1999 (for the ARCMs) and 1953–1999 (for the AORCMs)

	E	P	E − P	R	B	WB
ARCMs (2020–2049)	**[0, +8]**	*[−14, +4]*	**[+6, +17]**	*[−24, +3]*	*[−42, +17]*	**[+8, +35]**
Ensemble mean	**+4**	**−5**	**+12**	**−10**	**−13**	**+22**
AORCMs (2020–2049)	**[+1, +4]**	**[−12, −7]**	**[+8, +10]**	**[−22, −10]**	*[−10, +2]*	**[+15, +26]**
Ensemble mean	**+3**	**−10**	**+9**	**−16**	**−4**	**+20**
ARCMs (2070–2099)	**[+6, +18]**	**[−28, −4]**	**[+15, +35]**	**[−43, −5]**	*[−102, +25]*	**[+20, +60]**
Ensemble mean	**+12**	**−16**	**+25**	**−24**	**−40**	**+40**
CMIP3 (2070–2099)	**[+6, +9]**	*[−23, +2]*	**[+11, +25]**	**[−87, −56]**	**[−85, −63]**	**[+34, +42]**
Ensemble mean	**+7**	**−10**	**+18**	**−71**	**−74**	**+38**

Nonsignificant changes are in italics and significant changes in bold. CMIP3 values are from Mariotti et al. (2008). The ARCMs values are from Sanchez-Gomez et al. (2009). See text for details.

30-year periods, 2020–2049 and 2070–2099 (only for the ARCMs), as compared with the 1950–1999 period (1953–1999 for the AORCMS). To estimate the uncertainty interval, we consider the 90th percentile for the significance level to compute the lower and upper levels. The ARCMs show already significant changes for the 2020–2049 period, indicating an increase of E − P and total freshwater deficit. The AORCMs show significant changes for all fluxes except the Black Sea discharge. The strongest significant alterations of the Mediterranean hydrological cycles appear at the end of twenty-first century. The amplitude of the mean changes shown by CMIP3 and ARCMs for 2070–2099 is equivalent for all the terms in the water budget, except for B and R, whose representation by CMIP3 is not very realistic. The ARCM and AORCM experiments show a significant decrease of R, which corresponds to a decrease in terrestrial water resources, and an increase in salinity in the Mediterranean Sea. The AORCMs are coupled, but it is worth noting that in some of the models, the land-surface runoff is not interactive, and thus changes in the river discharge are not taken into account in the fluxes sent to the ocean.

The ensemble means for the AORCMS simulate an increase of freshwater deficit of 22% by 2050 and for both ARCMs and GCMs ~40% by 2100. The uncertainty associated with these changes is larger for ARCMs than for CMIP3, indicating that for ARCMs there is an additional source of uncertainty in the choice of the driving GCMs (Déqué et al., 2005). The uncertainty associated with these changes is reduced by the AORCMs as compared with ARCMs. The time series of water-budget components and freshwater loss averaged over the Mediterranean Sea show significant trends (Figures 8.14 and 8.15), indicating that global warming induces changes in the hydrological variables starting from around 2050, and that these changes become even stronger at the end of twenty-first century, according to Giorgi and Bi (2009) and Giorgi and Lionello (2008).

What is important to highlight here is that the future evolution of the water-budget components is oriented to an increase in the freshwater loss—i.e., an increase of evaporation, and decrease of precipitation, river discharge, and Black Sea discharge. Both CMIP3 and RCMs simulate a progressive drying of the Mediterranean region, nevertheless a large uncertainty still remains in the future climate projections.

8.4.3 Heat Budget

Under global-warming conditions, the surface temperatures simulated by climate models show an increase; thus, this induces changes in surface fluxes. The Mediterranean Sea, because of its semi-enclosed basin, should have, over long periods of time, a balance between the net surface heat flux and the heat transport through the Strait of Gibraltar (supposing that the Mediterranean heat content does not significantly vary under climate-change conditions). Over the past period this hypothesis is verified because the heat content over the Mediterranean has increase by only $0.4\,W/m^2$ over the 1950–2000 period (Rixen et al., 2005). Therefore, a strong constraint is imposed on the basin mean heat loss at the Mediterranean Sea surface, since it should compensate the net positive heat transport through the Strait of Gibraltar (of approximately $5\,W/m^2$ from mooring measurements). This constraint provided by the Strait of Gibraltar is the so-called heat-budget closure hypothesis.

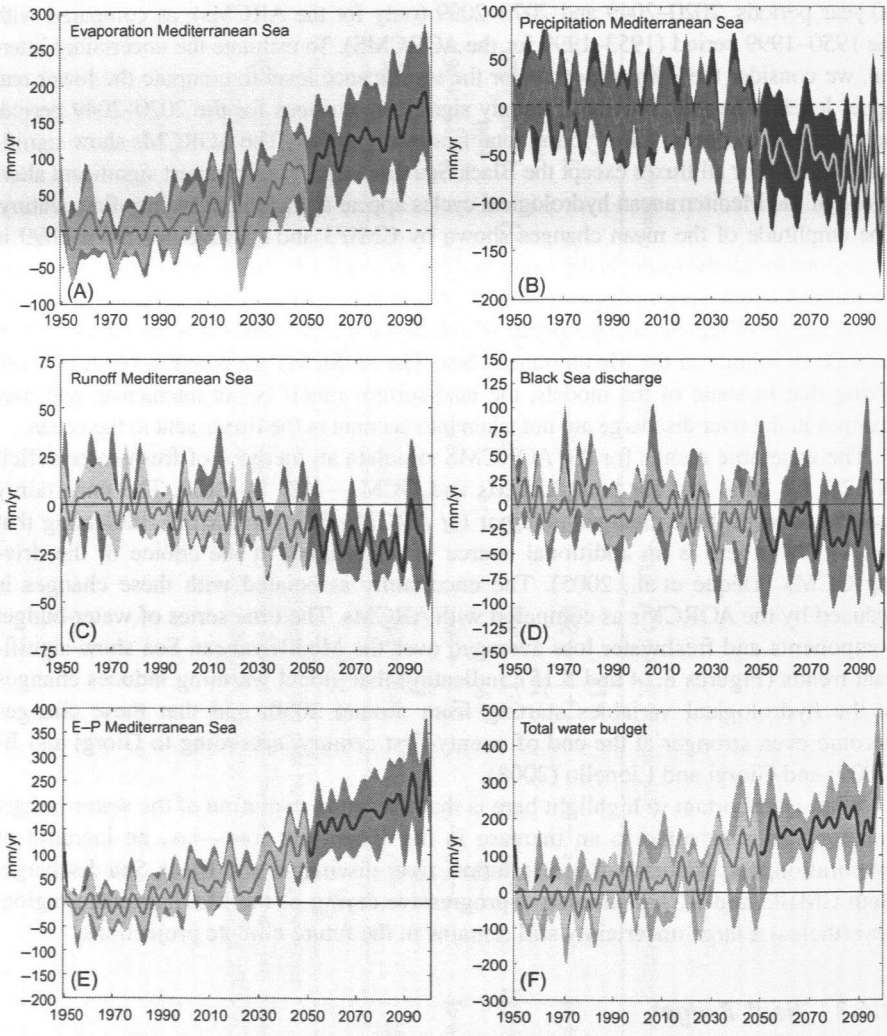

Figure 8.14 Time series of anomalies averaged over the whole Mediterranean Sea for the water-budget components, E–P, and total water budget from the ENSEMBLES project ("runoff" here stands for river discharge). The anomalies have been computed for the period 1950–2099 as compared with 1950–1999. From 1950 to 2050, 12 ARCMs were available, whereas only 7 ARCMs were available until 2099. The solid line represents the multimodel ensemble mean (for 12 and 7 ARCMs) filtered to remove periods shorter than 5 years. The colored shading indicates the levels of uncertainty.
Source: From Sanchez-Gomez et al. (2009).

The surface fluxes have been analyzed by Ruiz et al. (2008) from a high-resolution data set issued from a dynamical downscaling performed with the RCM REMO, forced at its boundaries by the NCEP/NCAR reanalysis (the so-called HIPOCAS data set, Sotillo et al., 2005). They showed that the heat-budget estimates

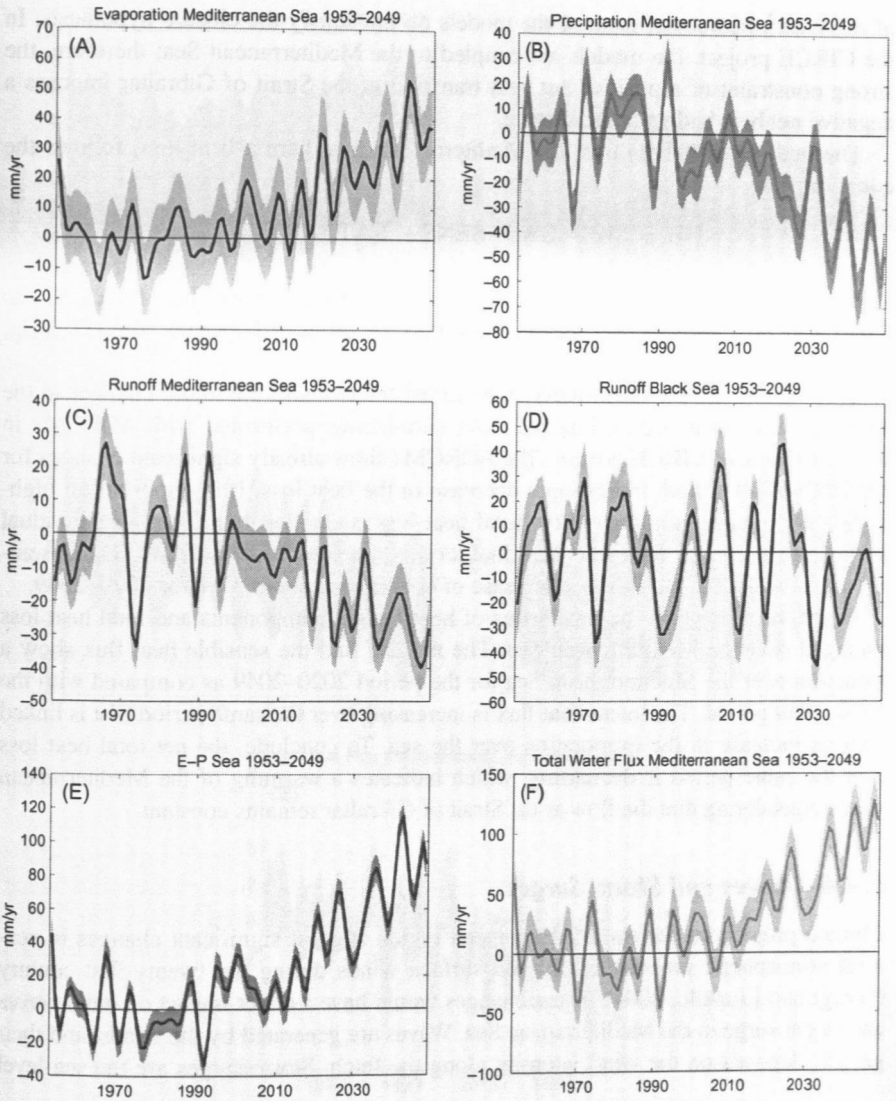

Figure 8.15 Same as in Figure 8.14. The anomalies have been computed for the period 1953–2049 as compared with 1953–1999 from five AORCMs from the CIRCE project. The solid line represents the multimodel ensemble mean filtered to remove periods shorter than 5 years. The colored shading indicates the levels of uncertainty.

from HIPOCAS satisfied the closure hypothesis better than the NCEP/NCAR reanalysis. In addition, Sanchez-Gomez et al. (2011) found, for the ARCMs from the ENSEMBLES project, very large discrepancies among the models for the heat-budget estimates. They vary from $-40\,W/m^2$ to $+21\,W/m^2$, with an ensembles mean

of $-9\,W/m^2$. Moreover, most of the models do not satisfy the closure hypothesis. In the CIRCE project, the models are coupled to the Mediterranean Sea; therefore, the strong constraint of a positive net heat transport at the Strait of Gibraltar imposes a negative net heat budget at the surface.

The heat budget (HB) over the Mediterranean Sea, here a heat loss, follows the equation:

$$HB = SW - LW - SENS - LAT \approx HT_{Gibraltar}$$

where SW is the shortwave, LW the longwave, SENS the sensible heat flux, LAT the latent heat flux, and the heat transport through the Strait of Gibraltar. The $HT_{Gibraltar}$ is $\sim 5\,W/m^2$.

Table 8.4 shows the uncertainty intervals associated with the future changes in the Mediterranean heat budget inferred from simulations performed with AORCMs in the framework of CIRCE project. The AORCMs show already significant changes for the 2020–2049 period, indicating a decrease in the heat loss. It is important to highlight that the uncertainty about the total heat loss is smaller than for each individual term, and the change for each individual term is not significant by 2049. The ensemble mean for AORCMs shows a decrease of heat flux of about 77% for 2020–2049.

Figure 8.16 displays the time series of heat-budget components and total heat loss averaged over the Mediterranean Sea. The net LW and the sensible heat flux show a reduction over the Mediterranean Sea for the period 2020–2049 as compared with the 1953–1999 period. The latent heat flux is increasing over the same period that is linked with an increase in the evaporation over the sea. To conclude, the net total heat loss over the same period is decreasing, which indicates a warming of the Mediterranean water, considering that the flow at the Strait of Gibraltar remains constant.

8.4.4 Waves and Storm Surges

Climate projections for the Mediterranean region suggest significant changes in sea-level atmospheric pressure (SLP) and surface winds during the twenty-first century (Giorgi and Lionello, 2008). These changes would have a direct impact on wind waves and storm surge in the Mediterranean Sea. Waves are generated by the winds, and their growth depends on the wind intensity along the fetch. Storm surges are the sea-level

Table 8.4 Percentages of Area-Averaged Mean Changes in the Mediterranean Sea for Shortwave (SW), Longwave (LW), Sensible Heat Flux (SENS), Latent Heat Flux (LAT), and Total Heat Budget (HB) for the Period 2020–2049 as Compared with 1953–1999

	SW	LW	SENS	LAT	HB
AORCMs (2020–2049)	*[−2, +4]*	*[−6, +2]*	*[−23, +4]*	*[−1, +7]*	**[−133, −21]**
Ensemble mean	**+1**	**−2**	**−9**	**+3**	**−77**

Nonsignificant changes are in italics and significant changes in bold. See text for details.

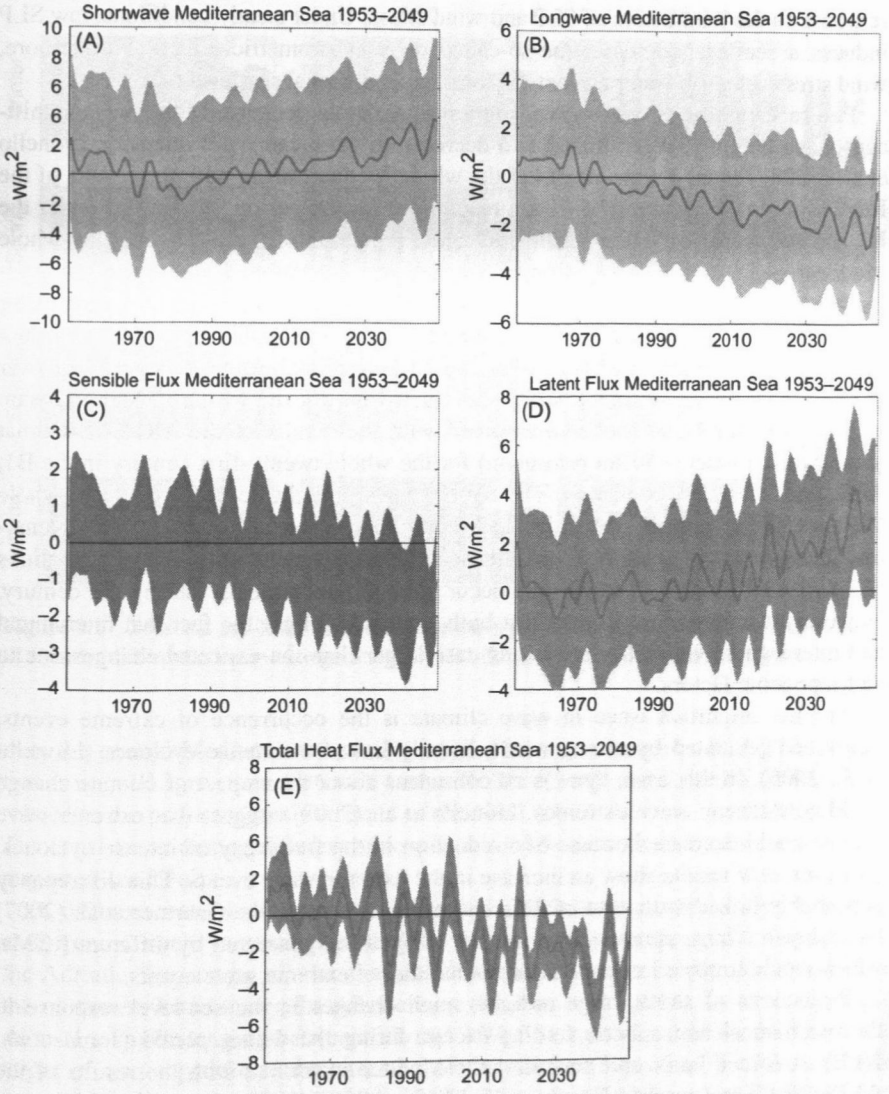

Figure 8.16 Time series of anomalies averaged over the whole Mediterranean Sea for the heat-budget components and total heat budget. The anomalies have been computed for the period 1953–2049 as compared with 1953–1999. Five AORCMs were available from the CIRCE project. The solid line represents the multimodel ensemble mean filtered to remove periods shorter than 5 years. The colored shading indicates the levels of uncertainty. (For interpretation of the references to color in this figure legend, the reader is referred to the web version of this book.)

response to the joint action of SLP and wind stress. Under steady conditions, low SLP induces a sea-level increase (the so-called inverse barometric effect). Furthermore, wind stress can push water against the coast, inducing local sea-level rise.

Future scenarios of wind waves suggest a moderate decrease of the mean significant wave height (SWH), linked to a decrease in the mean wind intensity. Lionello et al. (2008) forced a wave model of the whole Mediterranean with the results of the RegCM atmospheric model (~50 km resolution) for the period 2070–2100 under the B2 and A2 scenarios. Their results indicate a reduction of the SWH over the whole Mediterranean, except in the Alboran Sea, where it increases. The changes are especially significant during the winter season. The expected decrease is larger under the A2 scenario than under the B2 scenario, being moderate (~10–15% of reduction in the seasonally averaged SWH) in some regions but barely significant over most of the domain. A similar study was carried out for the western Mediterranean. In that case, the wave model was forced with the results of the ARPEGE-Climat atmospheric model (~50 km resolution) for the whole twenty-first century in the B1, A1B, and A2 SRES scenarios. The SWH shows a slight decrease over the whole Western Mediterranean, except in the Alboran Sea, where it increases in all scenarios. Changes would again be more intense with larger greenhouse-gas concentrations (A2 and A1B scenarios) and would occur almost monotonically during the century. However, it is important to note that both studies highlight the fact that interannual and interdecadal variability are in any case larger than the expected changes due to anthropogenic factors.

Another important issue in wave climate is the occurrence of extreme events. These are generated by strong winds, usually linked to intense cyclones (Lionello et al., 2006). In this case, there is no consensus about the impact of climate change on Mediterranean wave extremes. Lionello et al. (2008) suggest that extreme wave events would decrease because of a reduction in the frequency of intense cyclones. However, new results show an increase in the extreme wave events. This discrepancy is probably linked to the use of different atmospheric models. Gaertner et al. (2007) have shown a large spread in the number of cyclones generated by different RCMs, which would imply a large spread in the number of extreme wave events.

Projections of storm surge indicate small changes in the sea-level response to the mechanical atmospheric forcing except during the winter period (Jordà et al., 2012). A forced barotropic model of the Mediterranean Sea with the results of the ARPEGE-Climat model (Herrmann and Somot, 2008) exhibits changes in the sea-level PDF under all scenarios and over the whole domain, namely, an increase in the frequency of negative events and a decrease in the frequency of positive events (Marcos et al., 2011). These changes are induced by a decrease in the winter mean sea level and a slight increase in summer sea level (Figure 8.17). The maximum winter decrease would reach 8 cm at the end of the century in the A2 scenario, while the summer increase would be only 1 cm. Spring and autumn can be considered as transitional seasons with intermediate changes. Differences from the present climate are larger in the central and western Mediterranean, while in the Levantine basin they are negligible. This result is directly linked to changes in the SLP patterns. In this case, the ARPEGE-Climat model simulates an increase in the winter SLP, especially

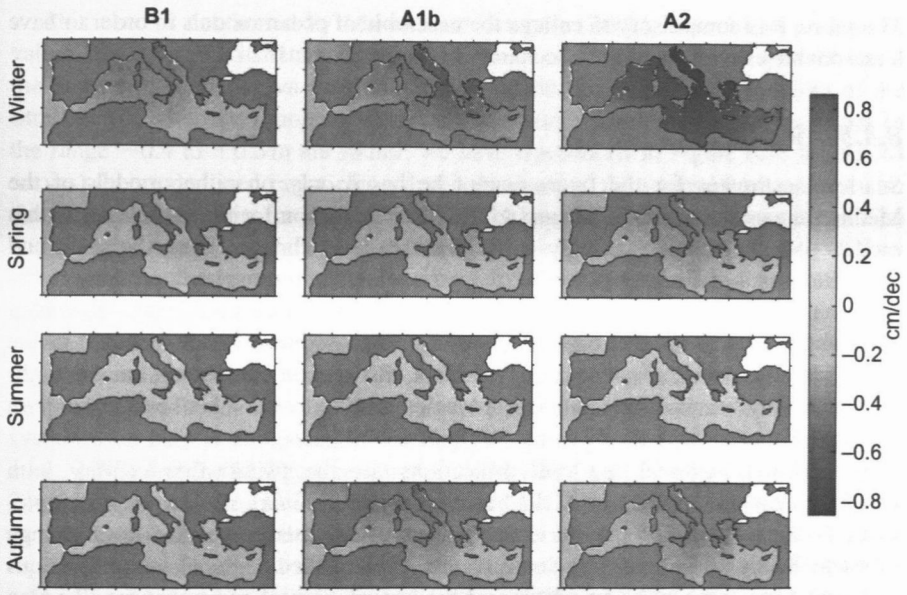

Figure 8.17 Seasonal sea-level trend (in centimeters per decade) induced by changes in the SLP under different climate-change scenarios: B1 (left), A1B (center) and A2 (right).

over the central Mediterranean, and a small decrease in summer SLP. This projection is in good agreement with many other RCMs (Giorgi and Lionello, 2008) and is related to the projected positive trend of the NAO (North Atlantic Oscillation) index. The consistency among different atmospheric models increases the confidence on the projected sea level.

A different issue is the projected change in storm-surge extreme events. In that case, return levels increase in the western basin and decrease in the Aegean and the Adriatic Seas under all the considered scenarios. Larger values are obtained in the northwest basin under the A2 scenario (Marcos et al., 2011). In all cases, variations are small, ranging between 0% and 15%. The northern Adriatic has been the target of some specific studies because of the vulnerability of its shallow northern coast (Lionello et al., 2003b, 2005, 2010). This set of studies also accounted for sea-level rise and has been based on scenarios and winds from two different RCMs. Results failed to suggest any clear future change of extreme surge levels, the intrinsic variability of the events being larger than the climate-change signal. However, as pointed out above, extreme events of storm surge are linked to the passage of intense cyclones, which is sensitive to the RCM used to force the ocean model. Therefore, the conclusions must be made with caution.

The wind wave and storm-surge projections obtained so far are a good starting point. However, it is important to note that they are based on a very limited number of experiments. Different authors (Gaertner et al., 2007) have pointed out the spread in the results of different RCMs and their sensitivity to changes in the forcings.

Therefore, it is compulsory to enlarge the ensemble of ocean models in order to have a reasonable estimation of the uncertainty of the projections.

8.4.5 Sea Level

Sea-level estimates for the future cannot be based only on either models of the Mediterranean Sea or AOGCMs and AORCMs. The reason for this deficiency is that models provide estimates of only one part of sea-level change. Thus, the steric and circulation-caused changes as well as the parts related to atmospheric pressure redistribution over the globe can be estimated (Marcos and Tsimplis, 2008). However, the component of sea-level change caused by mass addition is not included in the models and has to be added separately. In fact, this second component has the highest uncertainty because the nonlinear processes leading to ice-sheet breaking are not well understood.

In addition, regional sea-level projections for the twenty-first century with Mediterranean sea models or AORCMs are very preliminary. Below, as a complement to the estimate of the steric component of Mediterranean Sea-level change given in Section I.16, we give some results of published regional sea projections that include in some cases an estimate of the contribution of mass changes. We also describe with more detail one recent estimate of the contribution to Mediterranean Sea-level change from Mediterranean Sea incurred temperature and salinity changes calculated with an AORCM. For this specific study, steric or mass changes come from the nearby Atlantic, thus accounting for continental ice melting, are not included in the overall estimate of the trends.

The results of the simulation consisting of the forcing of the NEMOMED8 Mediterranean Sea model with the outputs of a high-resolution atmósphere-only climate-change SRES A2 scenario reported in Section 6.4.1 (Sevault et al., 2009) was also used to infer a projected sea-level change. First, the terms due to the steric and dynamics effects have been calculated from the temperature- and salinity-simulated changes. These contributions, which are revealed to be negative on average over the Mediterranean Sea, have been added to the global rise linked to continental ice melting, estimated as (+0.40, +2.00) cm per decade (IPCC, 2007). Thus, the obtained total sea-surface height trend for the Mediterranean Sea is expected to be between −0.08 and +1.52 cm per decade during the twenty-first century.

The results of the AORCM SRES A2 climate-change simulation presented in Section 8.4.1 (Somot et al., 2008) were also analyzed in terms of steric sea-level change (Tsimplis et al., 2008). The main finding is a mean steric sea-level rise of ~13 cm over the twenty-first century but with a significant spatial variability, with higher values in the western part of the basin. When the maximum value of the sea-level rise is 25 cm, coastal values are generally smaller than the mean. When adding estimated contributions from the atmospheric pressure change (−2 cm), melting of glaciers and ice sheets (−7 cm to +18 cm), and circulation effects (−6 cm to +6 cm), the resulting upper limit of mean sea-level rise over the twenty-first century given by this scenario is 35 cm. The authors of the study point out that a range of climate-change scenarios has to be considered to improve the uncertainty estimate.

This need is confirmed by Marcos and Tsimplis (2008), who found a range of values based on AOGCM simulations that are much larger. It can be up to 60 cm if the halosteric changes that they consider uncertain because of the modeling of the Strait of Gibraltar are ignored. When the halosteric changes are included, values in the range −0.4 to +0.5 m are found. We have reproduced in Figure 8.18 (AOGCM curves) their calculated range of sea-level change over the twenty-first century with the SRES A2 scenario for the thermosteric, halosteric, and steric components. The authors give more weight to the thermosteric component and consider the halosteric component more uncertain because of the deficient way of parameterizing the exchange of salt at the Strait of Gilbraltar.

Another estimate for the steric component of Mediterranean Sea-level change is obtained from a climate simulation performed with a regional ocean–atmosphere-coupled model and is also shown in Figure 8.18 (AORCM curves). The coupled system used here is composed of the RegCM3 atmospheric regional model (Giorgi et al., 1993) and the MITgcm ocean model (Marshall et al., 1997a,b; Sannino et al., 2009) coupled via the OASIS3 driver at 6 h intervals. The coupled model represents an improved version of that presented by Artale et al. (2010). The improvements regard the use of the natural boundary conditions for the freshwater flux in the oceanic component and the interactive calculation of the river discharges, including also the net inflow from the Black Sea, in the atmospheric component.

A 100-year simulation has been performed for the period 1951–2050. Lateral boundary conditions for the atmospheric component are extracted from the global coupled simulation performed by ECHAM5/MPI-OM model for the IPCC Fourth Assessment. The global climate model consists of the ECHAM5 AGCM (Roeckner et al., 2003) coupled to the ocean model MPI-OM (Marsland et al., 2003). The integration is performed at a resolution of T63L32 for the atmosphere and 1 × 1° of horizontal resolution and

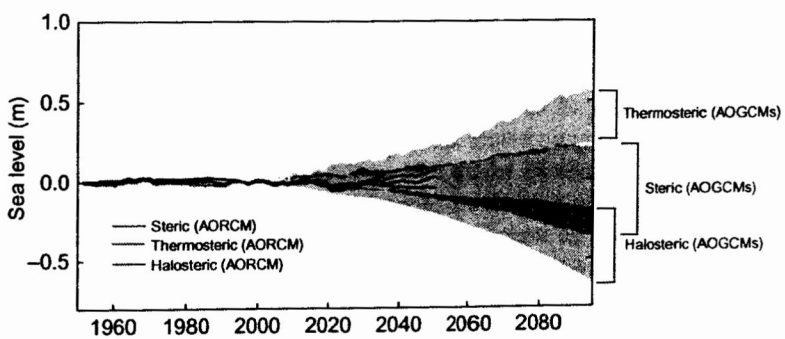

Figure 8.18 Various projections for sea-level change in the Mediterranean Sea. The AOGCM curves correspond to the thermosteric, halosteric, and steric components calculated by Marcos and Tsimplis (2008) for the SRES A2 scenario. The AORCM curves correspond to the same components calculated with a regional ocean–atmosphere-coupled model for the SRES A1B scenario. These results must be adjusted upward for the highly uncertain mass addition. See text for further details.

41 vertical levels for the oceanic component. For the first 50 years, the global simulation considers concentrations of CO_2, CH_4, and N_2O specified at observed values, while for the period 2001–2050 the SRES A1B scenario has been used.

Climatological monthly means of temperature and salinity (Levitus, 1982) have been adopted as lateral boundary conditions for the first 50 years of simulation in the ocean component of the RCM. For the scenario simulation, temperature and salinity monthly anomalies computed from the global simulation have been added to the Levitus monthly means.

Sea-level anomalies have been computed separately for the steric, thermosteric, and halosteric components. Values shown in Figure 8.18 (AORCM curves) are computed on the whole depth and averaged over the entire Mediterranean basin. The analysis of the present climate part of the simulation has shown a linear trend of temperature higher than that observed in a reference regional coupled simulation, where ERA40 data were used as boundary conditions. Considering this trend as a drift of the coupled system, the linear trend computed on the present climate simulation has been subtracted to the entire 100-year period. Figure 8.18 shows an increase of the steric component of the sea level during the scenario period due to the warming of the Mediterranean Sea and partially balanced by salinification.

The difference between the steric sea level computed over the last and the first 5 years of the scenario simulation (2001–2050) has a mean value on the basin of 1.4 cm. The sea level increases in the easternmost Mediterranean, the Aegean Sea, and the central basin, with a maximum of ~16 cm reached in the southern Adriatic basin. Large negative zones cover both the western and the eastern basins. Salinity contribution is everywhere negative, while temperature change implies an increase of sea level in most of the basin, with the exception of the western Mediterranean.

As compared with the AOGCM curves reported in Figure 8.18, the AORCM results give a lower range of variability. Apart from the fact that the SRES scenarios are different, this might also possibly be due to the lack of the global thermal expansion in the AORCM evaluation.

The model sea-level change estimates that are presented in this section and in the Introduction show that the steric effect of the temperature and salinity changes in the Mediterranean Sea over this century can yield positive or negative sea-level trends depending on whether temperature or salinity dominates. The trends are also spatially dependent, with regions where this steric component might be either positive or negative, whatever the sign of the mean trend. However, most part of the uncertainty on sea level change comes from the evaluation of the mass-change component. This includes sea-ice melting, but also to mass exchange between the nearby Atlantic and the Mediterranean Sea through the Strait of Gilbraltar. These terms are not estimated with the models and they are particularly uncertain because the contribution of continental ice melting is poorly known. As an overall conclusion for this section, the negative halosteric effect is generally much smaller than the currently predicted value of the positive contribution due to ice melting. Uncertainties need further investigation by understanding the exchange characteristics at the Strait of Gibraltar. Better characterization of the land ice-melting component and the circulation effects is also needed.

For the sea-level projections from models to become useful for coastal planning purposes, the mass addition of water from ice sheets needs to be resolved. This is an issue for the global sea level, and Mediterranean studies cannot add much to this. Also, land movements play a dominant part in sea-level change around the basin; thus, they need to be integrated in any projections for regional or local changes. The difficulties in understanding the dominant mechanisms by which ice sheets provide water to the oceans has led to the development of statistical modeling of sea-level change. These are based on an assumption that the response of sea level to changes in global atmospheric temperature are going to be linear in part of the transition period (Rahmstorf, 2007; Vermeer and Rahmstorf, 2009), which led to estimates of sea-level change of up to 1.8 m for the twenty-first century. Such global estimates have been combined for the Mediterranean Sea with land movements by Lambeck et al. (2010). While at present it is impossible to disprove the validity of such estimates, it must be very clear that they are statistical estimates based on a very simple relationship between atmospheric temperature and sea level and ignore the complex physics of air–sea interaction. Thus, their validity is strongly disputed (IPCC, 2010).

8.5 The Uncertainties of the Projections

Three main sources of uncertainties are impacting the assessment of climate-change projections. The first is related to the natural climate variability that remains unpredictable at the decadal and higher timescales. One way to deal with this uncertainty is to perform ensembles of simulations with varying initial conditions in order to sample the chaotic behavior of the climate system. The second one is associated with the modeling of the climate but can be of different origins. It can come from the so-called structural uncertainty that is related to the way processes are represented within models because some are lacking, others are poorly known, or because they are represented through imperfect equations. But modeling error can also come from input parameters and data that need to be specified, in particular in the parameterization of subgrid scale processes (e.g., cloud optical properties and land cover). One way to deal with modeling uncertainty consists of using multimodel ensembles that cover a sufficiently wide range of modeling hypotheses over key aspects of climate variability that are particularly uncertain. A method consisting of generating ensembles of simulations through a perturbation of input parameters has also been developed (Murphy et al., 2004). In this case, the ensemble was generated by perturbing uncertain physical parameters within plausible ranges but in a single model. The third main source of uncertainty is related to the choice of the emission scenario, since, as stated above, families of anthropogenic emission scenarios have been proposed by IPCC WGIII, encompassing a wide range of hypotheses. One way to deal with this type of uncertainty is, of course, to perform simulations with different emission scenarios.

But, in the case of regional climate modeling using RCMs, as part of the structural uncertainty it might be convenient to try to separate the relative contribution of

the structural uncertainty of the RCMs and the one associated with the choice of the AOGCMs used to prescribe their boundary conditions. Such an attempt was made by Déqué et al. (2007), who evaluated the four sources of uncertainties using the ensemble of PRUDENCE simulations through a variance analysis focusing on the climate change between 2071–2100 and 1961–1990. As a result, they found that the contribution of each source varies according to the climate variable, the region, and the season. However, one robust finding was that the role of the boundary conditions on the uncertainty is always dominant, whereas the contribution of climate variability is the weakest. This emphasizes the need to complete as much as possible the matrix using as entries different RCMs on one hand and different associated forcing AOGCMs on the other.

This was the case with the wider combination of RCMs and AOGCMs used in the ENSEMBLES project. Within the context of this project, a new analysis of the relative contribution of the different sources of uncertainty confirmed the dependence of the results according to the variable, the region, and the season (Goodess et al., 2009). For the Mediterranean area, and climate change between 2021–2050 and 1961–1990, the contribution of the forcing AOGCMs is generally similar to the contribution of the RCMs, with the exception of winter precipitation where AOGCMs dominate. This is different from the PRUDENCE results, but this could be at least partly due to the fact that these results concern the end of the century when the anthropic signal is stronger. The third contribution to the uncertainty comes from internal climate variability.

The wider matrix of the regional climate-change simulations of the ENSEMBLES project also allowed several evaluations of PDFs of temperature and precipitation changes. Some of them were constructed by taking into account a weighting of model results according to a metric developed within the framework of the project. A Gaussian kernel method was in particular applied to the ensemble of projections at a location close to Madrid (Goodess et al., 2009). It is here also applied using the same ensemble of simulations in Rome (Figure 8.19) and in Athens (Figure 8.20).

By construction, these PDFs include not only a representation of model structural uncertainties but also part of the uncertainty due to internal climate variability through a specific procedure using the daily values of the reference period 1961–1990. As demonstrated by Déqué and Somot (2010), the method is revealed to be relatively insensitive to the choice of the weighting procedure. As we can see in Figures 8.19 and 8.20, the sign of the precipitation change is uncertain in winter at the two locations and in autumn for Athens. Even in summer, the probability of observing an increase of precipitation is far from being negligible, as the spread is relatively large. On the contrary, the sign of the temperature change is always positive.

Other methods for constructing PDFs have also been proposed using different ensembles of simulations. One method, reported by Goodess et al. (2009), is an extension of the reliability ensemble averaging approach (Xu et al., 2010) applied to CMIP3 ensemble. It produces, in particular, a bimodal autumn rainfall change over the Mediterranean for 2071–2100. Another is based on the combination of 10,000 simulations obtained with the above-mentioned method consisting of perturbing the physical parameters of one climate model (Murphy et al., 2009). It was, in particular, applied within the framework of the ENSEMBLES project to some impact studies

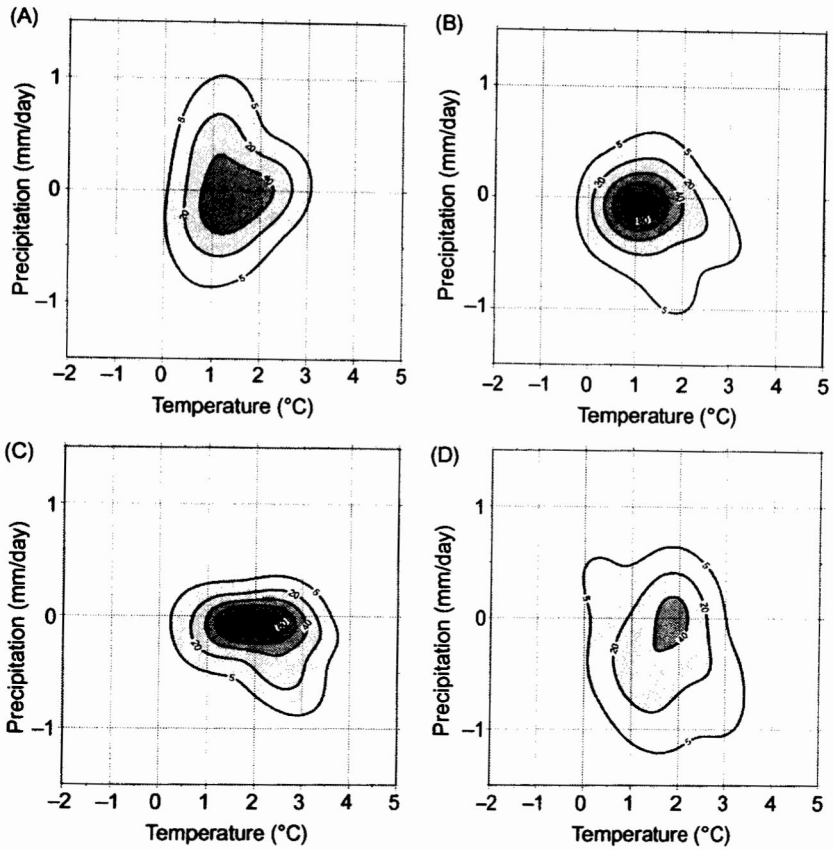

Figure 8.19 Bivariate PDFs for temperature and precipitation response (2021–2050 minus 1961–1990; A1B scenario) in Rome for DJF (A), MAM (B), JJA (C), and SON (D). Contours indicating densities are plotted for 5, 20, 40, 60, 80, and 100 of 10^{-2}/°C/mm/day.

over the Mediterranean area (Morse et al., 2009). Another approach applied to the PRUDENCE simulation ensemble method is based on a Bayesian approach (Buser et al., 2009). This variety of methods translates into an emerging research subject with a determination of probabilistic projections at the regional and even the local scale that is permitted by the development of a large ensemble of simulations. But it also draws attention to the fact that it is important to consider these constructed PDFs only as uncertain estimates of the true PDFs.

Apart from the use of large ensembles of simulations, an alternative approach of the uncertainty issue is also the one proposed by Rowell and Jones (2006) and then by Kendon et al. (2009) that consists of a mechanistic approach. The basic idea here is to determine the main mechanisms responsible for the simulated climate changes and then to attribute some subjective level of confidence on the projection according to the level of confidence we have for each of these dominant mechanisms. Through

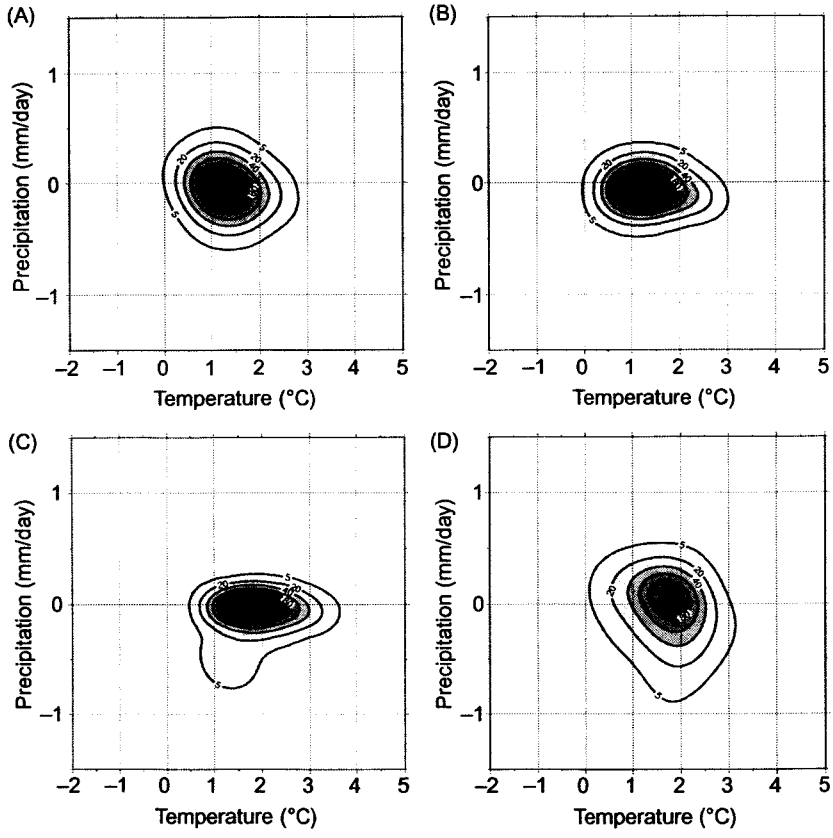

Figure 8.20 Same as Figure 8.19 for Athens.

an analysis of sensitivity experiments performed with an RCM of the Hadley Centre, Kendon et al. (2009) isolated in particular the contribution of warming, large-scale changes, spring soil-moisture decline, and summer soil-moisture feedback in driving precipitation change over Europe. They conclude in particular that in winter, warming is the dominant mechanism over much of Europe and that in summer, a decrease in mean precipitation over the Mediterranean area is also dominated by the warming mechanism but reinforced by the soil-moisture mechanisms. The important confidence in the warming mechanism thus reinforces the confidence we can have in the mean climate change over the region.

8.6 Conclusion

The level of confidence of future projections is of course dependent on the ability of models to reproduce the past and present climates. It is, however, a challenge

to define reliable metrics such as the one proposed within the framework of the ENSEMBLES project (see Section 8.5), since the link between a score based on the comparison of models to observations and the future climate change simulated by these models is far from being trivial. The development of process-oriented metrics for the processes that seem to play a dominant role in climate projections (like the cloud feedback on radiation budget) is a promising research activity. The application of models in the study of the detection and the attribution of climate change to different forcings is another one.

Detection is the process of demonstrating that climate has changed in some defined statistical sense, without providing a reason for that change. *Attribution* of causes of climate change is the process of establishing the most likely causes for the detected change with some defined level of confidence (IPCC, 2007). In practice, the responses to external forcing being calculated by models, a consistent detection, or attribution of different forcings in observations using different models tends to give some more confidence in the future climate simulated by these models.

Some studies conducted over southern Europe and over the Mediterranean region give some more insights on this issue. Stott et al. (2004) detected human influence on the temporal pattern of averaged summer temperatures over southern Europe, a region close to the Mediterranean area. Zhang et al. (2006) detected a spatiotemporal pattern of greenhouse and sulfate aerosol forcing on annual mean temperature over the same region and for the two periods 1900–1949 and 1950–1999. More recently, a formal analysis using new statistical methods (Ribes et al., 2009, 2010) allowed an extension of these previous results, since an anthropogenic signal is now detected not only for annual mean temperature over the Mediterranean area but also for summer and winter. In addition, some of the models of the CMIP3 database simulate a spatial pattern of change due to anthropogenic effects that is detected in the observation of the past few decades, even when this pattern is centered (i.e., when the temperature area mean is subtracted from the calculated signal). In addition, the application of a pattern similarity method developed in the context of the analysis of winter precipitation trends in northern Europe (Bhend and Von Storch, 2008), confirms the ability of the most part of CMIP3 models to reproduce the trends of temperature change over the domain over the 1979–2009 period and all the seasons, but with a slight underestimate in summer. This increases our confidence in temperature projections for those models that give the best agreement with observed temperature trends, and particularly their spatial pattern.

Unfortunately, this conclusion cannot be drawn for precipitation due to specific difficulties in detecting a signal of climate change on this variable. Further progress on this topic would require an improvement of the data sets of long series of homogenized observations and an improvement of the representation of hydrological processes in climate models.

Increasing our confidence in model projections implies also a specific attention to extreme climate events, since, as shown in this chapter, results might be to some extent contradictory, particularly in the case of storms. This implies that some progress should be accomplished in modeling such events with climate models and also in downscaling the results of model projections in order to reach a scale of

representation that is more suitable to reproduce this kind of events. The development of methods that rely on the nesting of a hierarchy of models of different levels of complexity, including nonhydrostatic models of a few kilometers of resolution, appears to be promising. But it is also challenging, considering the complexity of scale interaction and the requirement for high computing capacities that this implies.

Acknowledgments

S. Planton, C. Dubois, A. Elizalde, S. Gualdi, L. Li, P. Ruti, E. Sanchez-Gomez, F. Sevault, and S. Somot were partially supported by the EU FP6 IP CIRCE. Thanks to M. Déqué for providing Figures 8.19 and 8.20 and to the chapter reviewer for his very helpful comments. The authors also thank Dr. D. Jacob for her very helpful and constructive review.

References

Allen, M.R., 1999. Do-it-yourself climate prediction. Nature 401, 627.

Anav, A., Mariotti, A., 2011. Sensitivity of natural vegetation to climate change in the Euro-Mediterranean area. Clim. Res. 46, 277–292. doi: 10.3354/cr00993.

Anav, A., Ruti, P.M., Artale, V., Valentini, R., 2010. Modelling the effects of land-cover changes on surface climate in the mediterranean region. Clim. Res. 41, 91–104.

Andersson, A., Bakan, S., Fennig, K., Grassl, H., Klepp, C.-P., Schulz J., 2007. Hamburg ocean atmosphere parameters and fluxes from satellite data—HOAPS-3—monthly mean. World Data Center for Climate. doi:10.1594/WDCC/HOAPS3_MONTHLY.

Artale, V., Calmanti, S., Carillo, A., Dell'Aquila, A., Hermann, M., Pisacane, G., et al., 2010. An atmosphere-ocean regional climate model for the mediterranean area: assessment of a present climate simulation. Clim. Dyn. 35 (5), 721–740. doi: 10.1007/s00382-009-0691-8.

Baettig, M.B., Wild, M., Imboden, D.M., 2007. A climate change index: where climate change may be most prominent in the 21st century. Geophys. Res. Lett. 34, L01705. doi: 10.1029/2006GL028159.

Beniston, M., Stephenson, D.B., Christensen, O.B., Ferro, C.A.T., Frei, C., Goyette, S., et al., 2007. Future extreme events in European climate: an exploration of regional climate model projections. Clim. Change 81, 71–95. doi: 10.1007/s10584-006-9226-z.

Ben Rais Lasram, F., Guilhaumon, F., Albouy, C., Somot, S., Thuiller, W., Mouillot, D., 2010. The mediterranean sea as a "cul-de-sac" for endemic fishes facing climate change. Global Change Biol. 16 (12), 3233–3245. doi: 10.1111/j.1365-2486.2010.02224.x.

Bhend, J., von Storch, H., 2008. Consistency of observed winter precipitation trends in northern Europe with regional climate change projections. Clim. Dyn. 31, 17–28. doi: 10.1007/s00382-007-0335-9.

Bleu, P., 2009. State of the Environment and Development in the Méditerranean. ISBN: 978-92-807-3061-6. Job Number: DEP/1232/GR.

Boberg, F., Berg, P., Thejll, P., Gutowski, W.J., Christensen, J.H., 2009. Improved confidence in climate change projections of precipitation evaluated using daily statistics from the PRUDENCE ensemble. Clim. Dyn. 32, 1097–1106. doi: 10.1007/s00382-008-0446-y.

Buonomo, E., Jones, R., Huntingford, C., Hannaford, J., 2007. On the robustness of changes in extreme precipitation over Europe from two high resolution climate change simulations. Q. J. R. Meteorol. Soc. 133, 65–81.

Buser, C., Künsch, H.R., Lüthi, D., Wild, M., Schär, C., 2009. Bayesian multi-model projection of climate: bias assumptions and interannual variability. Clim. Dyn. 33, 849–868. doi: 10.1007/s00382-00ç-0588-6.

Christensen, J.H., Christensen, O.B., 2007. A summary of the PRUDENCE model projections of change in European climate at the end of this century. Clim. Change 81, 7–30.

Coppola, E., Giorgi, F., Rauscher, S.A., Piani, C., 2010. Model weighting based on mesoscale structures in precipitation and temperature in an ensemble of regional climate models. Clim. Res. 44, 121–134. doi: 10.3354/cr00940.

Déqué, M., Somot, S., 2010. Weighted frequency distributions express modelling uncertainties in the ENSEMBLES regional climate experiments. Clim. Res. 44, 195–209. doi: 10.3354/cr00866.

Déqué, M., Jones, R.G., Wild, M., Giorgi, F., Christensen, J.H., Hassell, D.C., et al., 2005. Global high resolution versus limited area model climate change projections over Europe: quantifying confidence level from PRUDENCE results. Clim. Dyn. 25, 653–670.

Déqué, M., Rowell, D.P., Lüthi, D., Giorgi, F., Christensen, J.H., Rockel, B., et al., 2007. An intercomparison of regional climate simulations for Europe: assessing uncertainties in model projections. Clim. Change 81, 53–70.

Elguindi, N., Somot, S., Déqué, M., Ludwig, W., 2010. Climate change evolution of the hydrological balance of the Mediterranean, Black and Caspian Seas: impact of climate model resolution. Clim. Dyn. 36 (1–2), 205–228. doi: 10.1007/s00382-009-0715-4.

Fouillet, A., Rey, G., Laurent, F., Pavillon, G., Bellec, S., Ghihenneuc-Jouyaux, C., et al., 2006. Excess mortality related to the August 2003 heat wave in France. Int. Arch. Occup. Environ. Health 80, 16–24. doi: 10.1007/s00420-006-0089-4.

Fowler, H.J., Ekstrom, M., Blenkinsop, S., Smith, A.P., 2007. Estimating change in extreme European precipitation using a multimodel ensemble. J. Geophys. Res. 112, D18104. doi: 10.1029/2007JD008619.

Frei, C., Schöll, R., Schmidli, J., Fukutome, S., Vidale, P.L., 2006. Future change of precipitation extremes in Europe: an intercomparison of scenarios from regional climate models. J. Geophys. Res. 111, D06105.

Gaertner, M., Jacob, D., Gil, V., Domınguez, M., Padorno, E., Sanchez, E., et al., 2007. Tropical cyclones over the mediterranean sea in climate change simulations. Geophys. Res. Lett. 34, L14711. doi: 10.1029/2007GL029977.

Gao, X., Pal, J., Giorgi, F., 2006. Projected changes in mean and extreme precipitation over the mediterranean region from a high resolution double nested RCM simulation. Geophys. Res. Lett. 33, L03706. doi: 10.1029/2005GL024954.

Giorgi, F., 2002. Variability and trends of sub-continental scale surface climate in the century. Part I: observations. Clim. Dyn. 18, 675–691.

Giorgi, F., Bi, X., 2009. Time of emergence (TOE) of GHG-forced precipitation change hotspots. Geophys. Res. Lett. 36, L06709. doi: 10.1029/2009GL037593.

Giorgi, F., Coppola, E., 2009. Projections of twenty-first century climate over Europe. Eur. Phys. J. Conf. 1, 29–46. doi: 10.1140/epjconf/e2009-00908-9.

Giorgi, F., Lionello, P., 2008. Climate change projections for the mediterranean region. Global Planet. Change 63, 90–104.

Giorgi, F., Bates, G., Nieman, S., 1993. The multi-year surface climatology of a regional atmospheric model over the western United States. J. Clim. 6, 75–95.

Goodess, C.M., Jacob, D., Déqué, M., Guttiérrez, J.M., Huth, R., Kendon, E., et al., 2009. Dowscaling methods, data and tools for input to impacts assessments. In: van der Linden, P., Mitchell, J.F.B. (Eds.), Summary of Research and Results from the ENSEMBLES Project. Met Office Hadley Centre, Exeter, UK, pp. 59–78.

Goubanova, K., Li, L., 2007. Extremes in temperature and precipitation around the mediterranean basin in an ensemble of future climate scenario simulations. Global Planet. Change 57, 27–42.

Held, I.M., Soden, B.J., 2006. Robust responses of the hydrological cycle to global warming. J. Clim. 19 (21), 5686–5699.

Herrmann, M., 2007. Formation et devenir des masses d'eau en Méditerranéen nord-occidentale. Influence sur l'écosystème planctonique pélagique. Variabilité interannuelle et changement climatique. Ph.D. Thesis. Toulouse III—Paul Sabatier University, Toulouse, France.

Herrmann, M., Somot, S., 2008. Relevance of ERA40 dynamical downscaling for modeling deep convection in the Mediterranean Sea. Geophys. Res. Lett. 35 (L04607), 1–5.

Herrmann, M., Estournel, C., Déqué, M., Marsaleix, P., Sevault, F., Somot, S., 2008. Dense water formation in the Gulf of Lion shelf: impact of atmospheric interannual variability and climate change. Cont. Shelf Res. 28 (15), 2092–2112.

Hertig, E., Jacobeit, J., 2008. Assessments of mediterranean precipitation changes for the 21st century using statistical downscaling techniques. Int. J. Climatol. 28, 1025–1045.

Hertig, E., Seubert, S., Jacobeit, J., 2010. Temperature extremes in the mediterranean area: trends in the past and assessments for the future. Nat. Hazards Earth Syst. Sci. 10, 2039–2050.

IPCC (Intergovernmental Panel on Climate Change), 2000. In: Nakicenovic, N., Swart, R. (Eds.), Emission Scenarios. A Special Report of IPCC Working Group III. Cambridge University Press, Cambridge, UK.

IPCC, 2007. In: Solomon, S., Qin, D., Manning, M., Chen, Z., Marquis, M., Averyt, K.B., et al. (Eds.), Climate Change 2007: The Physical Science Basis. Contribution of Working Group I to the Fourth Assessment Report of the Intergovernmental Panel on Climate Change. Cambridge University Press, Cambridge, UK.

IPCC, 2010. In: Stocker, T.F., Qin, D., Plattner, G.-K., Tignor, M., Allen, S., Midgley P.M. (Eds.), Workshop Report of the Intergovernmental Panel on Climate Change Workshop on Sea Level Rise and Ice Sheet Instabilities. IPCC Working Group I Technical Support Unit, University of Bern, Bern, Switzerland, p. 227.

Jordà, G., Gomis, D., Álvarez-Fanjul, E., Somot, S., 2012. Atmospheric contribution to Mediterranean sea level variability under different climate change scenarios. Global Planet. Change 80–81, 198–214. doi: 10.1016/j.gloplacha.2011.10.013.

Josey, S., Kent, E., Taylor, P., 1999. New insights into the ocean heat budget closure problem from analysis of the SOC air–sea flux climatology. J. Clim. 12, 2856–2880.

Kendon, E.J., Rowell, D.P., Jones, R.G., 2009. Mechanisms and reliability of future projected changes in daily precipitation. Clim. Dyn. 35 (2–3), 489–509.

Kharin, V.V., Zwiers, F.W., 2000. Changes in the extremes in an ensemble of transient climate simulations with a coupled Atmosphere–Ocean GCM. J. Clim. 13, 3760–3788.

Kharin, V.V., Zwiers, F.W., 2005. Estimating extremes in transient climate change simulations. J. Clim. 18, 1156–1173.

Lambeck, K., Antoniolic, F., Anzideid, M., Ferrantie, L., Leonic, G., Scicchitanof, G., et al., 2010. Sea level change along the Italian coast during the holocene and projections for the future. Quat. Int. 232 (1–2), 250–257.

Levitus, S., 1982. Climatological Atlas of the World Ocean. United States Government Printing, Rockville, Md., USA.

Li, L., Bozec, A., Somot, S., Béranger, K., Bouruet-Aubertot, P., Sevault, F., et al., 2006. Regional atmospheric, marine processes and climate modelling. In: Lionello, P., Malanotte-Rizzoli, P., Boscolo, R. (Eds.), Mediterranean Climate Variability. Elsevier, Amsterdam. (Chapter 7).

Lionello, P., Elvini, E., Nizzero, A., 2003a. Ocean waves and storm surges in the Adriatic Sea: intercomparison between the present and doubled CO_2 climate scenarios. Clim. Res. 23, 217–231.

Lionello, P., Martucci, G., Zampieri, M., 2003b. Implementation of a coupled atmosphere-wave-ocean model in the Mediterranean Sea: sensitivity of the short time scale evolution to the air–sea coupling mechanisms. Global Atmos. Ocean Syst. 9, 65–95.

Lionello, P., Mufato, R., Tomasin, A., 2005. Sensitivity of free and forced oscillations of the Adriatic Sea to sea level rise. Clim. Res. 29, 23–39.

Lionello, P., Bhend, J., Buzzi, A., Della-Marta, P.M., Krichack, S., Jansà, A., et al., 2006. Cyclones in the Mediterranean region: climatology and effects on the environment. In: Lionello, P., Malanotte-Rizzoli, P., Boscolo, R. (Eds.), Mediterranean Climate Variability. Elsevier, Amsterdam, pp. 325–372.

Lionello, P., Cogo, S., Galati, M.B., Sanna, A., 2008. The Mediterranean surface wave climate inferred from future scenario simulations. Global Planet. Change 63, 152–162. doi: 10.1016/j.gloplacha.2008.03.004.

Lionello, P., Galati, M.B., Elvini, E., 2010. Extreme storm surge and wind wave climate scenario simulations at the venetian littoral. Phys. Chem. Earth doi: 10.1016/j.pce.2010.04.001.

Lu, J., Vecchi, G.A., Reichler, T., 2007. Expansion of the Hadley cell under global warming. Geophys. Res. Lett. 34 (6), 5.

Ludwig, W., Dumont, E., Meybeck, M., Heussner, S., 2009. River discharges of water and nutrients to the Mediterranean Sea: major drivers for ecosystem changes during past and future decades? Prog. Oceanogr. 80, 199–217.

Marcos, M., Tsimplis, M.N., 2008. Comparison of AOGCMs in the Mediterranean Sea during the 21st century. J. Geophys. Res. 113, C12028.

Marcos, M., Jordà, G., Gomis, D., Pérez, B., 2011. Changes in storm surges in southern Europe during the 21st century. Global Planet. Change 77, 116–128. doi: 10.1016/j.gloplacha.2011.04.002.

Mariotti, A., Struglia, M.V., Zeng, N., Lau, K.M., 2002. The hydrological cycle in the Mediterranean region and implications for the water budget of the Mediterranean sea. J. Clim. 15, 1674–1690.

Mariotti, A., Zeng, N., Yoon, J., Artale, V., Navarra, A., Alpert, P., et al., 2008. Mediterranean water cycle changes: transition to drier 21st century conditions in observations and CMIP3 simulations. Environ. Res. Lett. doi: 10.1088/1748-9326/3/044001.

Marshall, J., Adcroft, A., Hill, C., Perelman, L., Heisey, C., 1997a. A finite-volume, incompressible Navier Stokes model for, studies of the ocean on parallel computers. J. Geophys. Res. 102, 5753–5766.

Marshall, J., Hill, C., Perelman, L., Adcroft, A., 1997b. Hydrostatic, quasi-hydrostatic, and nonhydrostatic ocean modeling. J. Geophys. Res. 102, 5733–5752.

Marsland, S.J., Haak, H., Jungclaus, J.H., Latif, M., Roske, F., 2003. The Max Planck Institute global/sea-ice model with orthogonal curvilinear coordinates. Ocean Model. 5, 91–127.

McGuffie, K., Henderson-Sellers, A., Holbrook, N., Kothavala, Z., Balachova, O., Hoekstgra, J., 1999. Assessing simulations of daily temperature and precipitation variability with global climate models for present and enhanced greenhouse climates. Int. J. Climatol. 19, 1–26.

Meehl, G.A., Zwiers, F., Evans, J., Knutson, T., Mearns, L., Whetton, P., 2000. Trends in extreme weather and climate events: issues related to modelling extremes in projections of future climate change. Bull. Am. Meteorol. Soc. 81, 427–436.

Morse, A., Prentice, C., Carter, T., 2009. Assessment of climate change impacts. In: van der Linden, P., Mitchell, J.F.B. (Eds.), Summary of Research and Results from the ENSEMBLES Project. Met Office Hadley Centre, Exeter, UK, pp. 107–129.

Murphy, J.M., Sexton, D.M.H., Barnett, D.N., Jones, G.S., Webb, M.J., Collins, M., et al., 2004. Quantification of modelling uncertainties in a large ensemble of climate change simulations. Nature 430, 768–772.

Murphy, J.M., Sexton, D.M.H., Jenkins, G.J., Boorman, P.M., Booth, B.B.B., Brown, C.C., et al., 2009. UK Climate Projections Science Report: Climate Change Projections. Met Office Hadley Centre, Exeter, UK.

Piani, C., Frame, D.J., Stainforth, D.A., Allen, M.R., 2005. Constraints on climate change from a multithousand member ensemble of simulations. Geophys. Res. Lett. 32, L23825. doi: 10.1029/2005GL024452.

Pope, V.D., Gallani, M.L., Rowntree, P.R., Stratton, R.A., 2000. The impact of new physical parameterizations in the hadley centre climate model, HadAMs. Clim. Dyn. 16, 123–146.

Previdi, M., Liepert, B.G., 2007. Annular modes and Hadley cell expansion under global warming. Geophys. Res. Lett. 34 (22), 5, L22701.

Rahmstorf, S., 2007. A semi-empirical approach to projecting future sea-level rise. Science 315, 68–370.

Ribes, A., Azaïs, J.-M., Planton, S., 2009. Adaptation of the optimal fingerprint method for climate change detection using a well-conditioned covariance matrix estimate. Clim. Dyn. 33, 707–722. doi: 10.1007/s00382-009-0561-4.

Ribes, A., Azaïs, J.-M., Planton, S., 2010. A method for regional climate change detection using smooth temporal patterns. Clim. Dyn. 35 (2–3), 391–406. doi: 10.1007/s00382-009-0670-0.

Rixen, M., Beckers, J.-M., Levitus, S., Antonov, J., Boyer, T., Maillard, C., et al., 2005. The western Mediterranean deep water: a proxy for climate change. Geophys. Res. Lett. 32, L12608. doi: 10.1029/2005GL022702.

Roeckner, E., Buml, G., Bonaventura, L., Brokopf, R., Esch, M., Giorgetta, M., et al., 2003. The Atmospheric General Circulation Model ECHAM5. Part I: Model Description, Tech. Rep. 349. Max-Planck Institute for Meteorology, Hamburg, Germany.

Roether, W., Manca, B., Klein, B., Bregant, D., Georgopoulos, D., Beitzel, V., et al., 1996. Recent changes in eastern Mediterranean deep waters. Science 271, 333–335.

Rohling, E.J., Hilgen, F.J., 1991. The eastern Mediterranean climate at times of sapropel formation: a review. Geologie en Mijnbouw 70, 253–264.

Rosenzweig, C., Casassa, G., Karoly, D.J., Imeson, A., Liu, C., Menzel, A., et al., 2007. Assessment of observed changes and responses in natural and managed systems. In: Parry, M.L., Canziani, O.F., Palutikof, J.P., van der Linden, P.J., Hanson, C.E. (Eds.), Climate Change 2007: Impacts, Adaptation and Vulnerability. Contribution of Working Group II to the Fourth Assessment Report of the Intergovernmental Panel on Climate Change. Cambridge University Press, Cambridge, UK, pp. 79–131.

Rowell, D.P., Jones, R.G., 2006. Causes and uncertainty of future summer drying over Europe. Clim. Dyn. 27, 281–299. doi: 10.1007/s00382-006-0125-9.

Ruiz, S., Gomis, D., Sotillo, M.G., Josey, S.A., 2008. Characterizatrion of surface heat fluxes in the Mediterranean Sea from a 44-year high-resolution atmospheric dataset. Global Planet. Change 63, 258–274.

Sanchez, E., Gallardo, C., Gaertner, M.A., Arribas, A., de Castro, M., 2004. Future climate extreme events in the mediterranean simulated by a regional climate model: a first approach. Global Planet. Change 44, 163–180.

Sanchez-Gomez, E., Somot, S., Mariotti, A., 2009. Future changes in the mediterranean water budget projected by an ensemble of regional climate models. Geophys. Res. Lett. 36, L21401. doi: 10.1029/2009Gl040120.

Sanchez-Gomez, E., Somot, S., Josey, S.A., Dubois, C., Elguindi, N., Déqué, M., 2011. Evaluation of Mediterranean sea water and heat budgets simulated by an ensemble of high resolution regional climate models. Clim. Dyn. doi: 10.1007/s00382-011-1012-6.

Sannino, G., Herrmann, M., Carillo, A., Rupolo, V., Ruggiero, V., Artale, V., et al., 2009. An eddy permitting model of the Mediterranean Sea with a two-way grid refinement at the Strait of Gibraltar. Ocean Model 30, 56–72. doi: 10.1016/j.ocemod.2009.06.002.

Schär, C., Vidale, P.L., Luthi, D., Frei, C., Haberli, C., Liniger, M.A., et al., 2004. The role of increasing temperature variability in European summer heatwaves. Nature 427, 332–336. doi: 10.1038/nature02300.

Seager, R., Ting, M.F., Held, I.M., Kushnir, Y., Lu, J., Vecchi, G., et al., 2007. Model projections of an imminent transition to a more arid climate in southwestern North America. Science 316 (5828), 1181–1184.

Semmler, T., Jacob, D., 2004. Modeling extreme precipitation events—a climate change simulation for Europe. Global Planet. Change 44 (1-4), 119–127.

Sevault, F., Somot, S., Beuvier, J., 2009. A regional version of the NEMO ocean engine on the Mediterranean Sea: NEMOMED8 user's guide. Technical Note 107. CNRM, Météo-France, Toulouse.

Somot, S., 2005. Modélisation climatique du bassin méditerranéen: variabilité et scénarios de changement climatique. Ph.D. Thesis. Toulouse III—Paul Sabatier University, Toulouse, France (in French).

Somot, S., Sevault, F., Déqué, M., 2006. Transient climate change scenario simulation of the Mediterranean Sea for the 21st century using a high-resolution ocean circulation model. Clim. Dyn. 27 (7–8), 851–879. doi: 10.1007/s00382-006-0167-z.

Somot, S., Sevault, F., Déqué, M., Crépon, M., 2008. 21st century climate change scenario for the Mediterranean using a coupled atmosphere–ocean regional climate model. Global Planet. Change 63 (2–3), 112–126. doi: 10.1016/j.gloplacha.2007.10.003.

Sotillo, M.G., Ratsimandresey, A.W., Carretero, J.C., Bentamy, A., Valero, F., González-Rouco, F., 2005. A high-resolution 44-year atmospheric hindcast for the Mediterranean Basin: contribution to the regional improvement of global reanalysis. Clim. Dyn. 25 (2–3), 219–236. doi: 10.1007/s00382-005-0030-7.

Stanev, E.V., Le Traon, P.Y., Peneve, E.L., 2000. Sea level variations and their dependency on meteorological and hydrological forcing: analysis of altimeter and surface data for the Black Sea. J. Geophys. Res. 105, 17203–17216.

Stott, P.A., Stone, D.A., Allen, M.R., 2004. Human contribution to the European heatwave of 2003. Nature 432, 610–614.

Taylor, K.E., Stouffer, R.J., Meehl, G.A., 2009. A summary of the CMIP5 Experiment Design. <http://cmip-pcmdi.llnl.gov/cmip5/docs/Taylor_CMIP5_design.pdf> .

Thorpe, R.B., Bigg, G.R., 2000. Modelling the sensitivity of Mediterranean outflow to anthropogenically forced climate change. Clim. Dyn. 16, 355–368.

Tsimplis, M., Marcos, M., Somot, S., 2008. 21st century Mediterranean sea level rise: steric and atmospheric pressure contributions from a regional model. Global Planet. Change 63 (2–3), 105–111. doi: 10.1016/j.gloplacha.2007.09.006.

Vermeer, M., Rahmstorf, S., 2009. Global sea level linked to global temperature. Proc. Natl. Acad. Sci. U.S.A. 106 (51), 21527–21532.

Vitolo, R., Ruti, P.M., Dell'Aquila, A., Felici, M., Lucarini, V., Speranza, A., 2009. Accessing extremes of mid-latitudinal wave activity: methodology and application. Tellus 61A, 35–49 C.

Xu, Y., Gao, X., Giorgi, F., 2010. Upgrades of the reliability ensemble averaging method for producing probabilistic climate change predictions. Clim. Res. 41, 61–81.

Zaitchik, B.F., Macalady, A.K., Smith, R.B., 2006. Europe's 2003 heat wave: a satellite view of impacts and land–atmosphere feedbacks. Int. J. Climatol. 26, 743–769. doi: 10.1002/joc.1280.

Zhang, X., Zwiers, F., Stott, P.A., 2006. Multimodel multisignal climate change detection at regional scale. J. Clim. 19, 4294–4307.